NASA Ames Research Center Contributions to the PADRI workshop

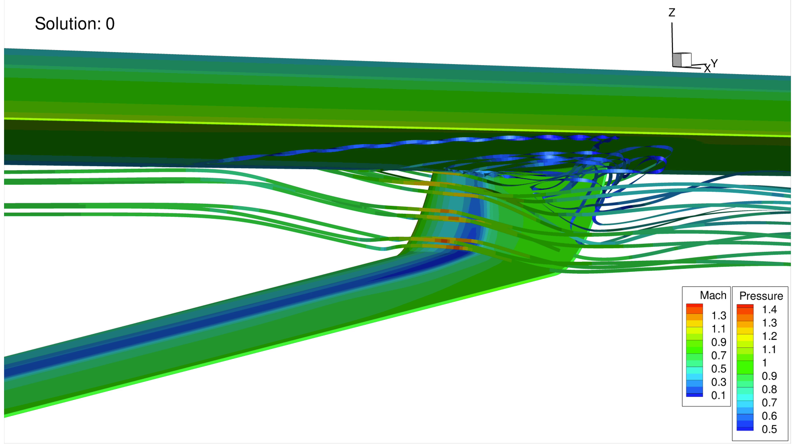

Gaetan Kenway
Jeffery Housman
Cetin Kiris

Computational Aerosciences Branch
NASA Ames Research Center

November 29, 2017

PADRI

- PADRI: A common platform for validation of aircraft drag reduction technologies
- Generic strut-braced wing configuration
- Slightly swept wing for low cruise Mach number (0.72)
- Simplified geometry without engines, empennage or flap-track fairings
- Significant wave-drag and flow separation at strut-wing intersection
- Focus of this workshop is to redesign the junction

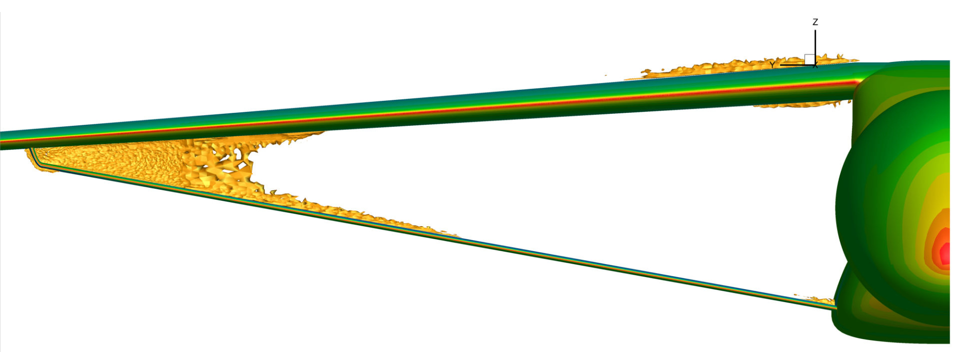

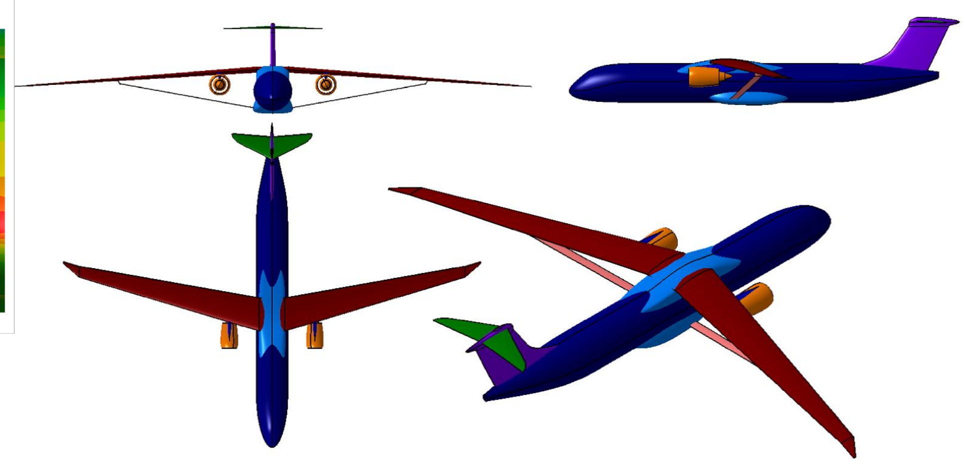

MDO for Aircraft Configurations with High-fidelity (MACH)

<table>
<tr><td colspan="4">Python user script
Setup up the problem: objective function, constraints, design variables, optimizer and solver options</td><td rowspan="1"></td></tr>
<tr><td colspan="2">Optimizer interface
pyOptSparse
Common interface to various optimization software</td><td colspan="2">Aerostructural solver
AeroStruct
Coupled solution methods and coupled derivative evaluation</td><td rowspan="2">Geometry modeler
DVGeometry/GeoMACH
Defines and manipulates geometry, evaluates derivatives</td></tr>
<tr><td>SNOPT</td><td>Other optimizers</td><td>Flow solver
ADflow
Governing and adjoint equations</td><td>Structural solver
TACS
Governing and adjoint equations</td></tr>
</table>

- Underlying solvers are parallelized and compiled
- All communication done through memory
- Easy-to-use Python scripting interface
- Only using aerodynamic design capacity for PADRI

ADFlow

- Automatic-Differentiation Flow Solver
- Second order finite volume RANS
- Standard SA turbulence model
- Point-matched multiblock and overset grids
- Multiple solvers: Runge Kutta (RK), DDADI, approximate Newton Krylov (ANK) and Newton Krylov (NK) algorithms
- DADI, ANK and NK used for optimization
- Extremely fast convergence for small design changes

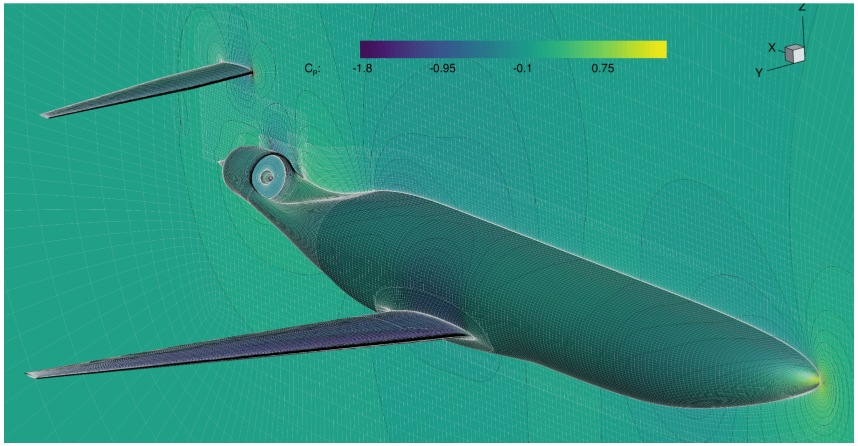

MIT D8 Double Bubble

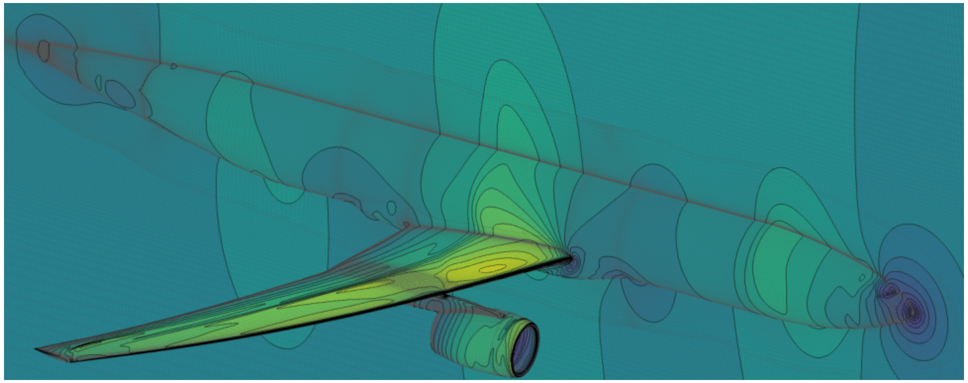
Common Research Model (DPW6)

ADFlow Solver Convergence

- Combination of three algorithms: Diagonalized Alternating Direction Implicit (DADI), Approximate Newton-Krylov (ANK) and Newton Krylov (NK)
- Newton-Krylov fully couples flow and turbulence variables

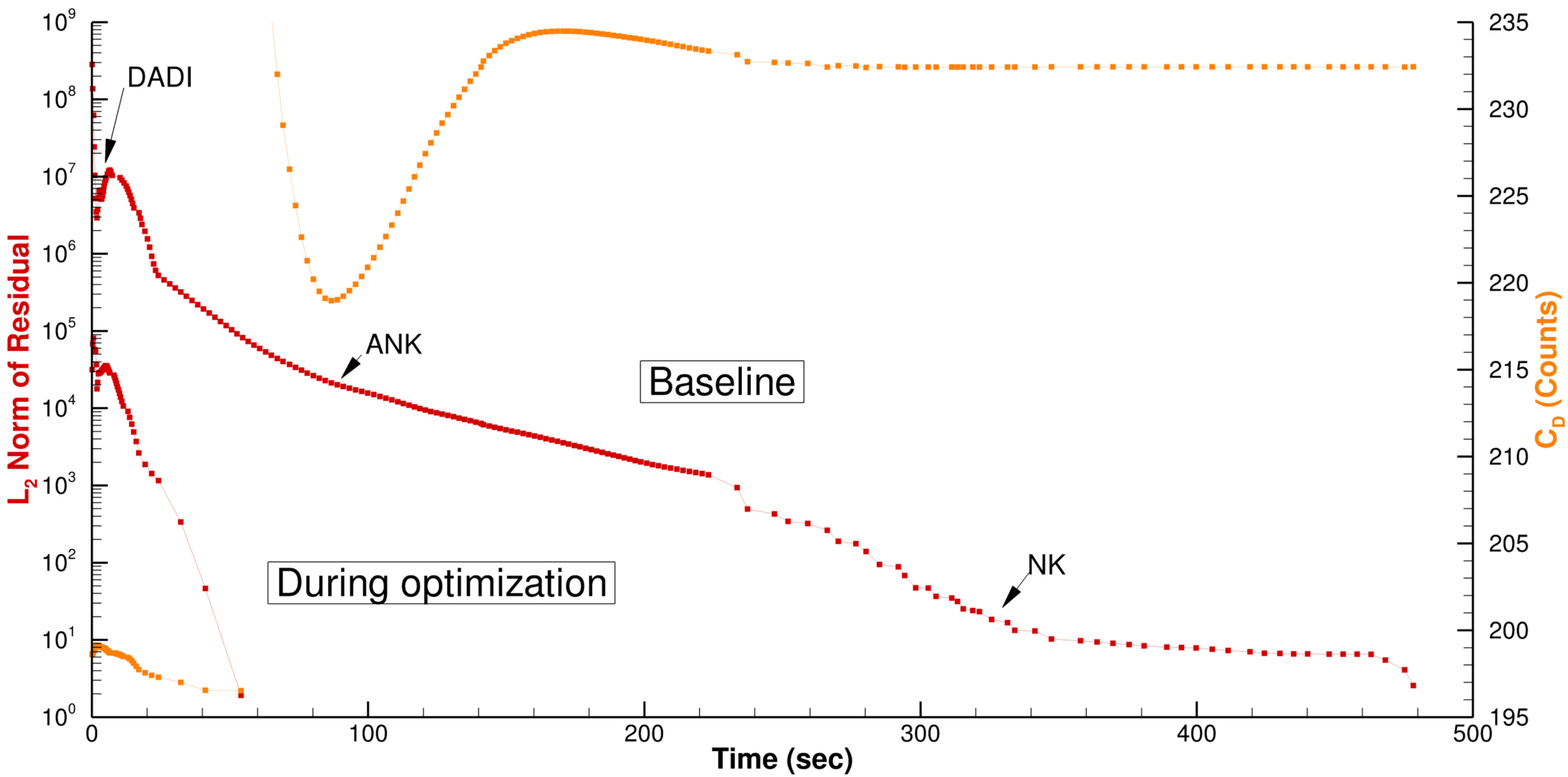

Mesh Deformation

- Inverse-distance weighting method
- Parallel, fast and highly robust for large deformations

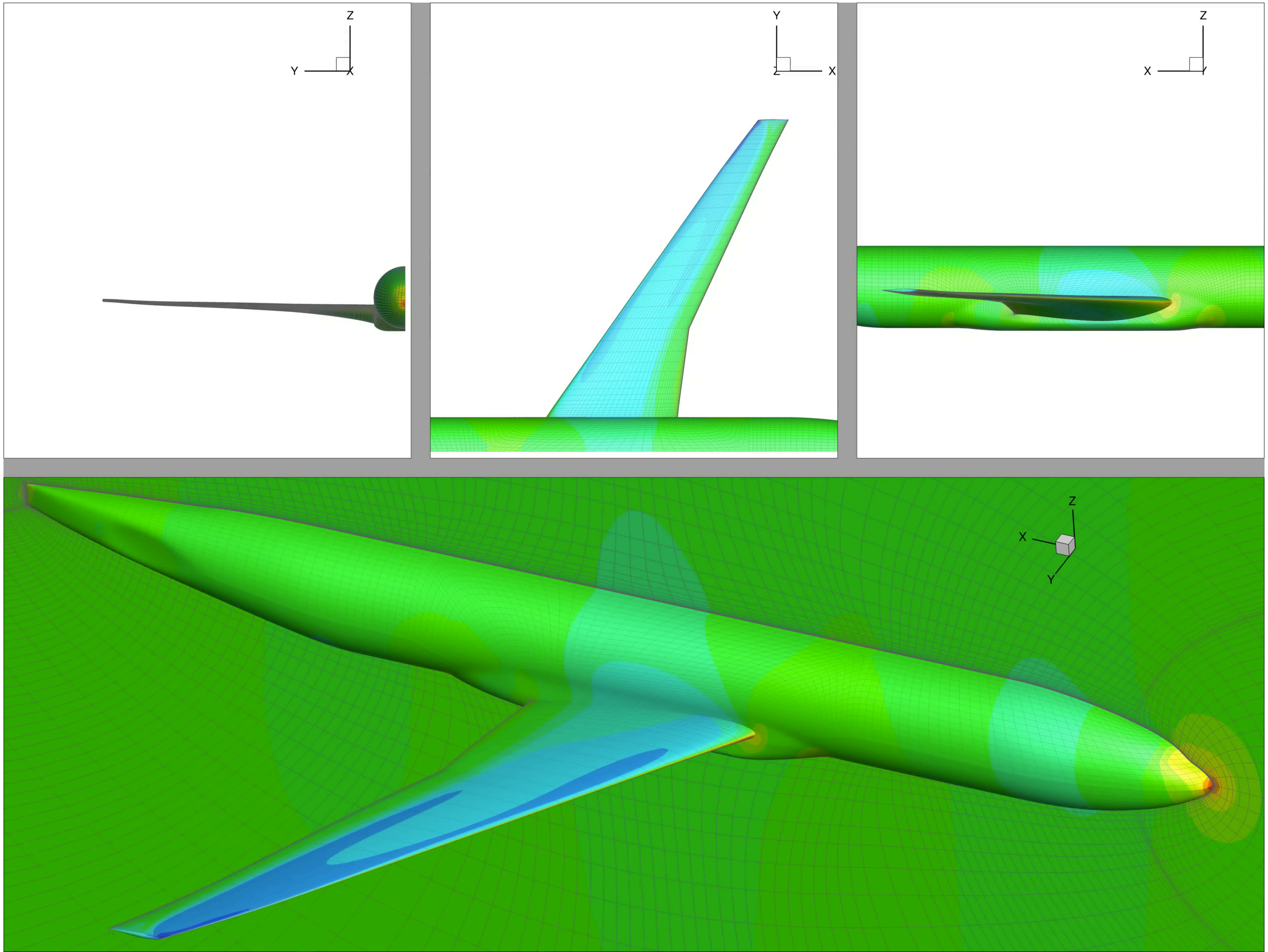

Geometry Manipulation

- Free-form deformation (FFD) volume approach
- Parametrize the change in geometry
- Embed discrete geometry into trivariate B-spline volumes
- Point-inversion algorithm to find u-v-w coordinates
- Control point motion smoothly controls the underlying geometry
- Sub-FFD approach for localized control

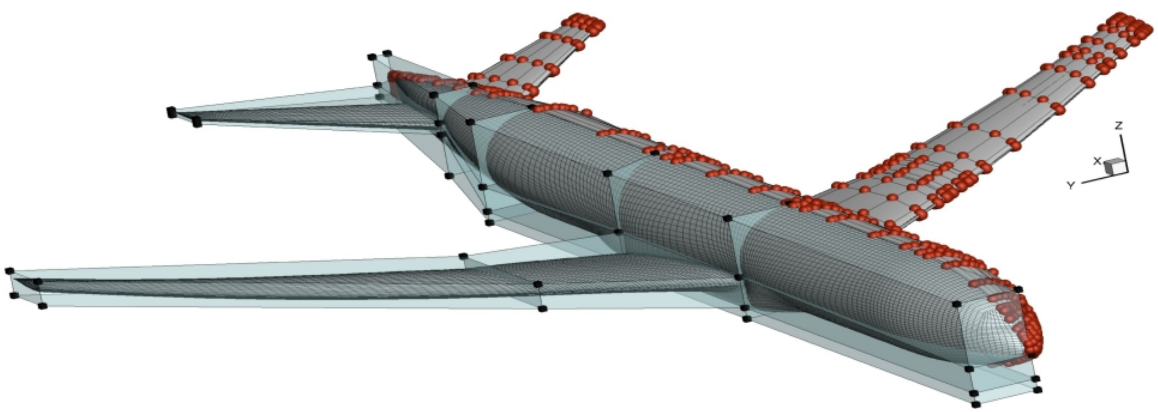

Overset Meshes

- Surface patches generated with Pointwise
- Chimera Grid Tools (CGT) for volumetric extrusion
- Hyperbolic mesh extrusion
- Consistent refinement between levels

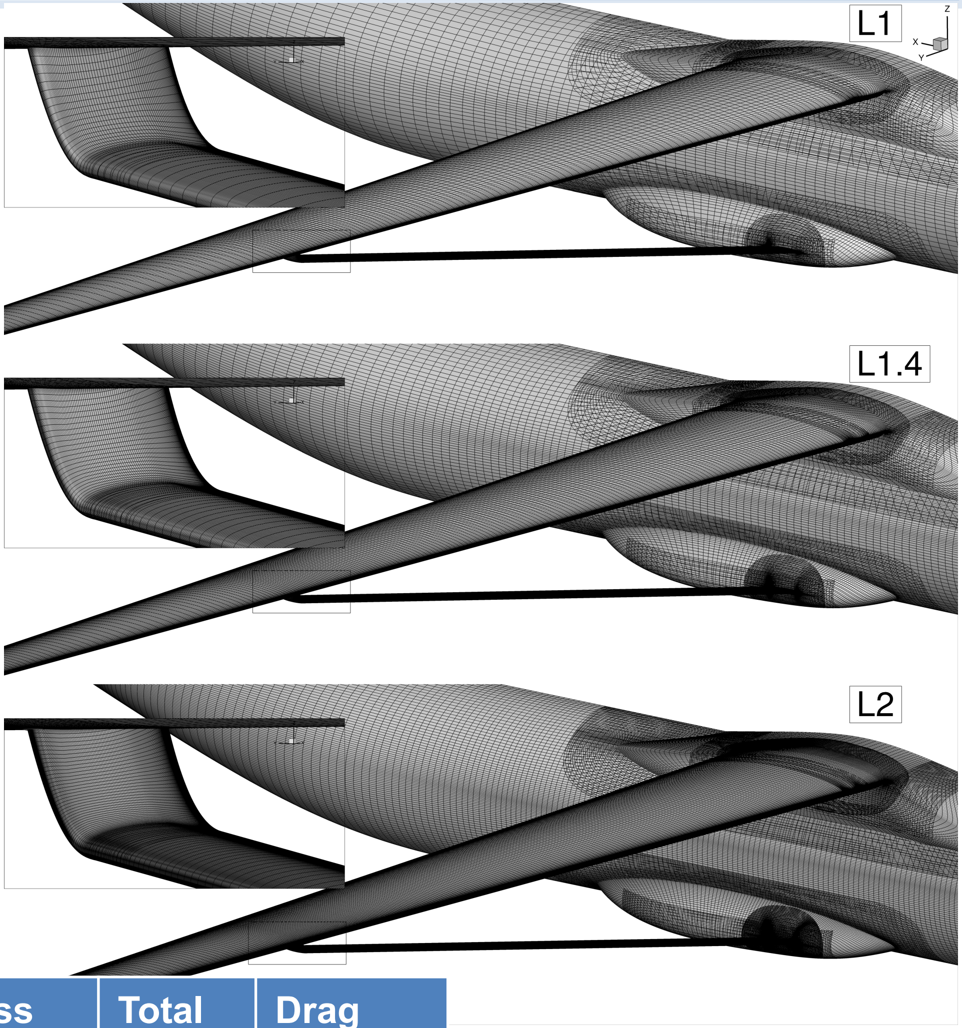

Mesh	# Wing Chordwise	# Wing Spanwise	# Truss Chordwise	# Truss Spanwise	Total Cells	Drag (counts)
L1	64	202	96	110	7.4 M	232.42
L1.4	88	282	134	154	19.2 M	224.61
L2	126	404	192	220	57.3 M	220.87

Baseline Configuration Grid Convergence

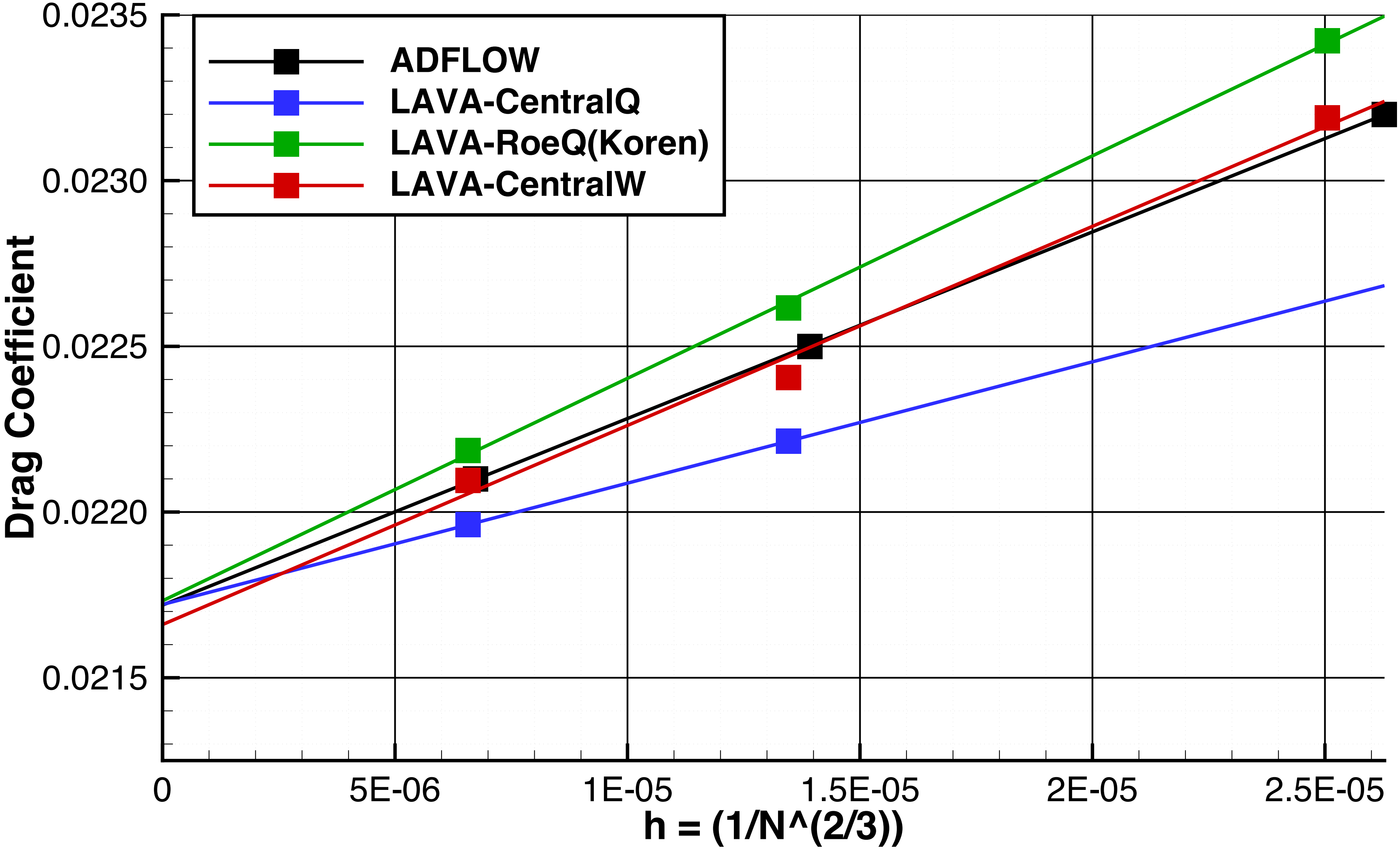

Baseline Solutions (Shock Sensor)

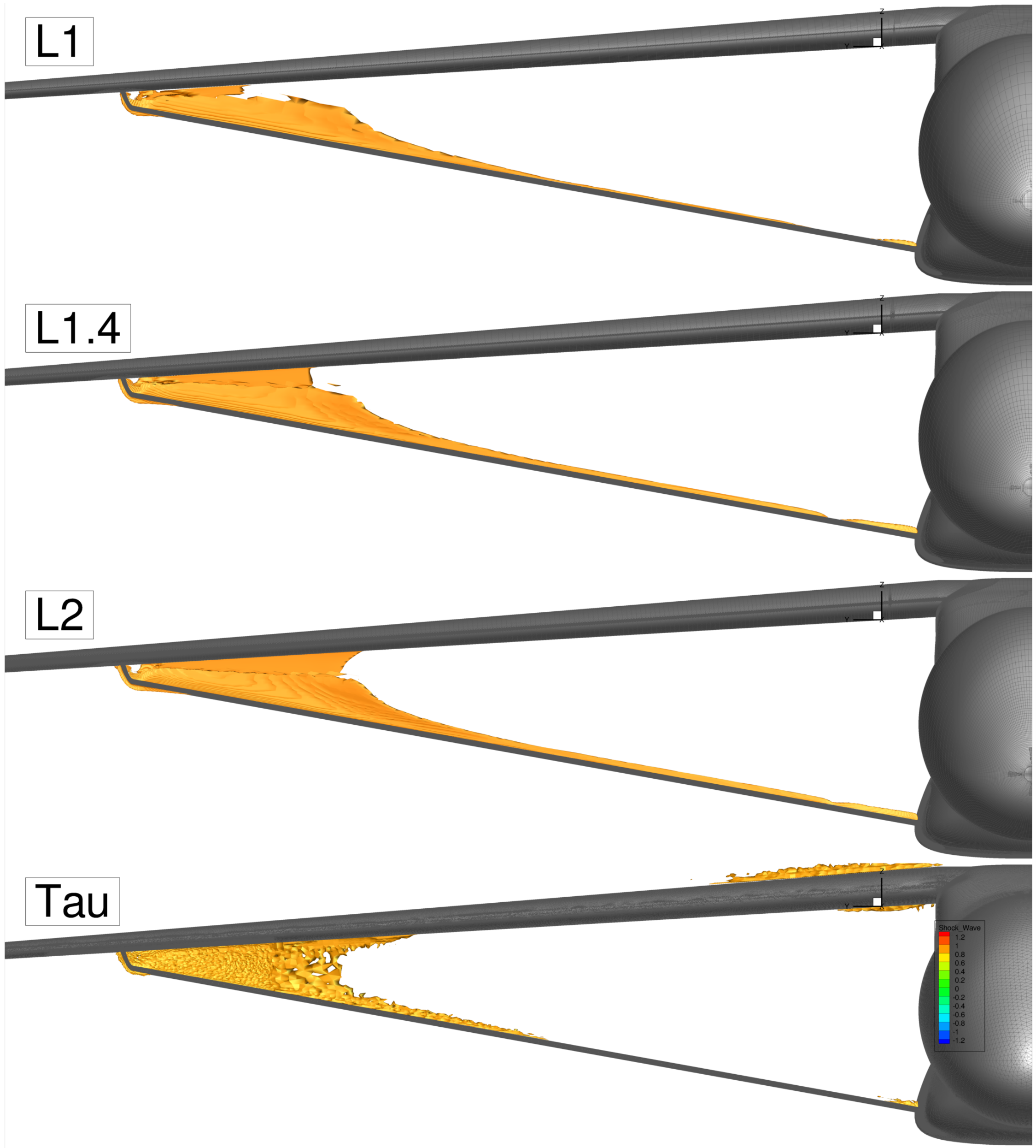

Optimization Problem Description

- Single point drag minimization (CL=0.417)
- Design Variables: FFD Shape position + angle of attack
- Flight condition: M=0.72, altitude=30,000 ft, alpha=1.0

- Case 1
- Nominal design problem

Case 2
- Nominal design problem + fixed trailing edge

Case 3
- Full truss redesign

Optimization Design Variables

- Only truss is modified
- Follows workshop guidelines for design region (Case 1 and 2)
- Orange control point sphere are modified

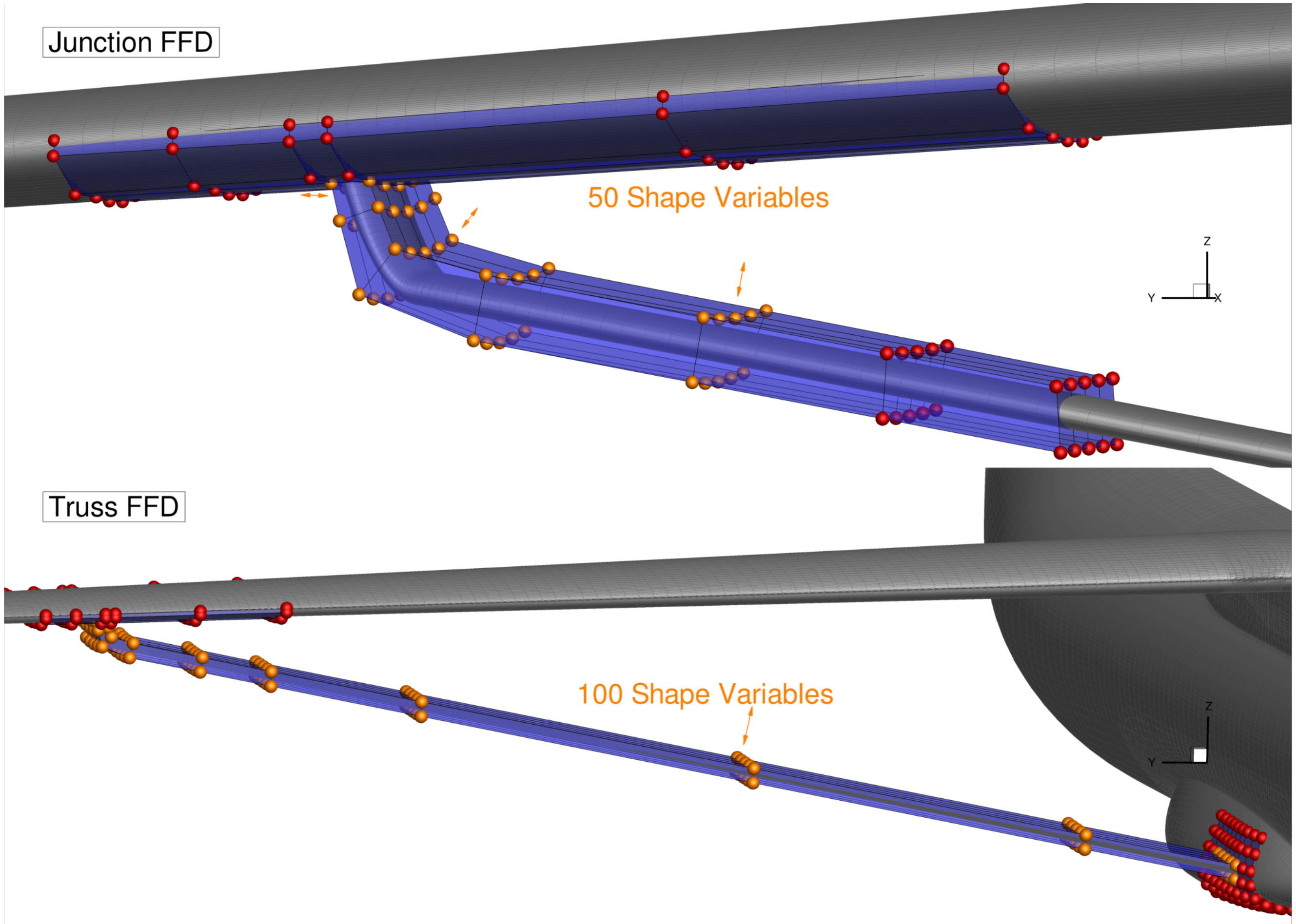

Optimization Constraints

- Explicit “toothpick” thickness constraints

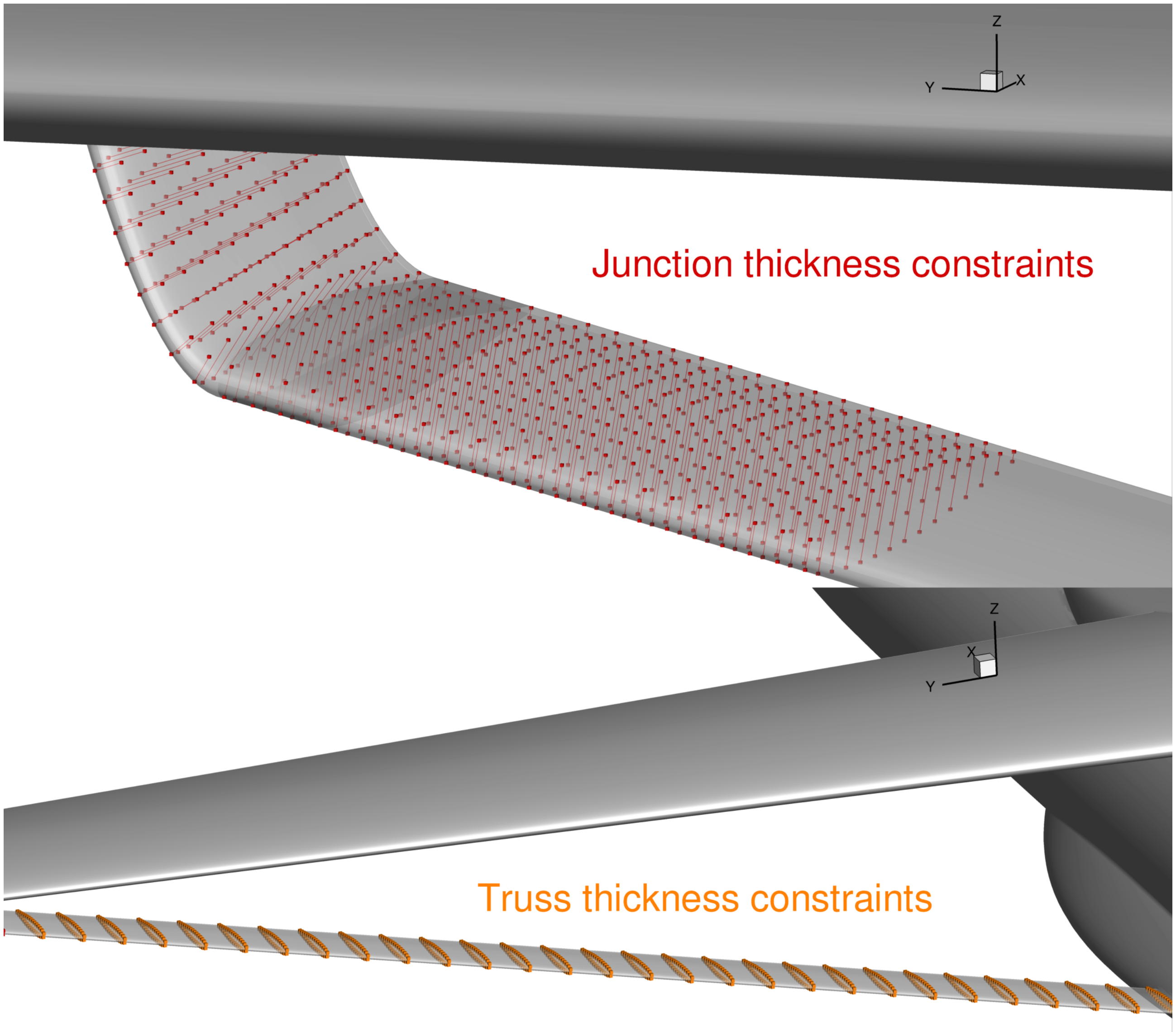

Optimization Constraints

- Linear constraints enforce fixed leading and (optionally) trailing edge
- These constraints are enforced exactly by the optimizer

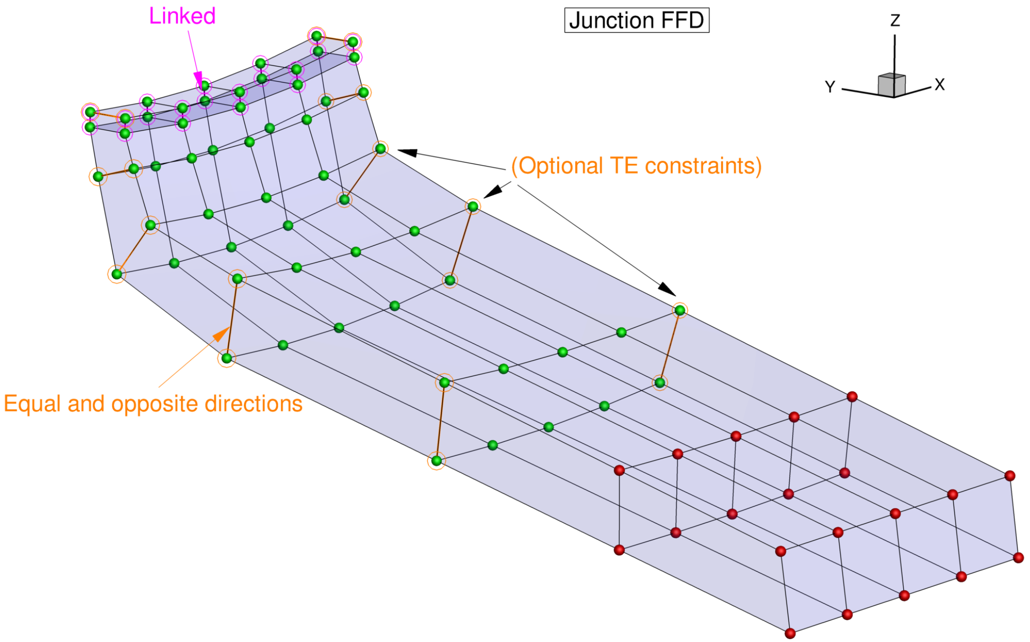

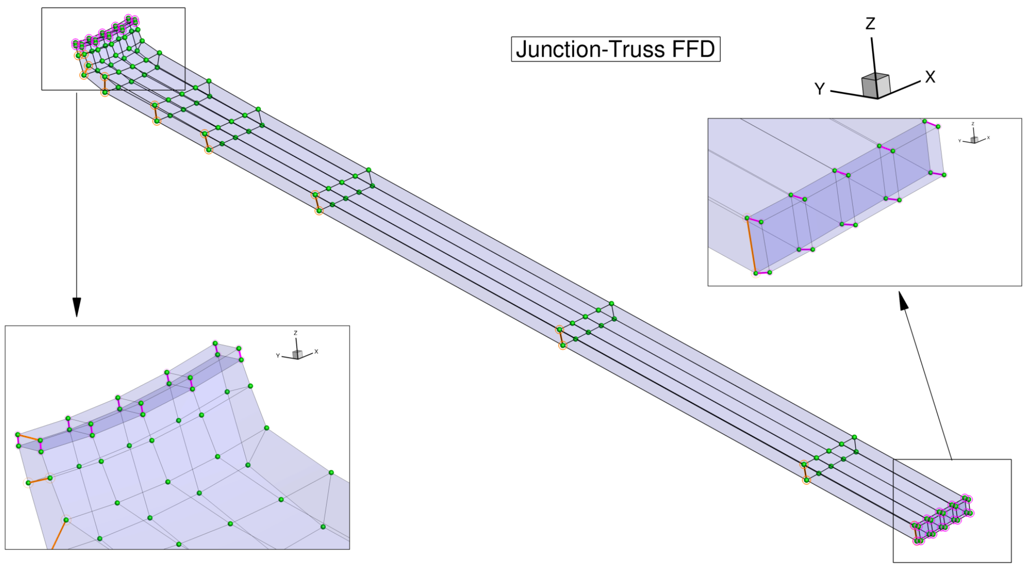

Optimization Convergence History

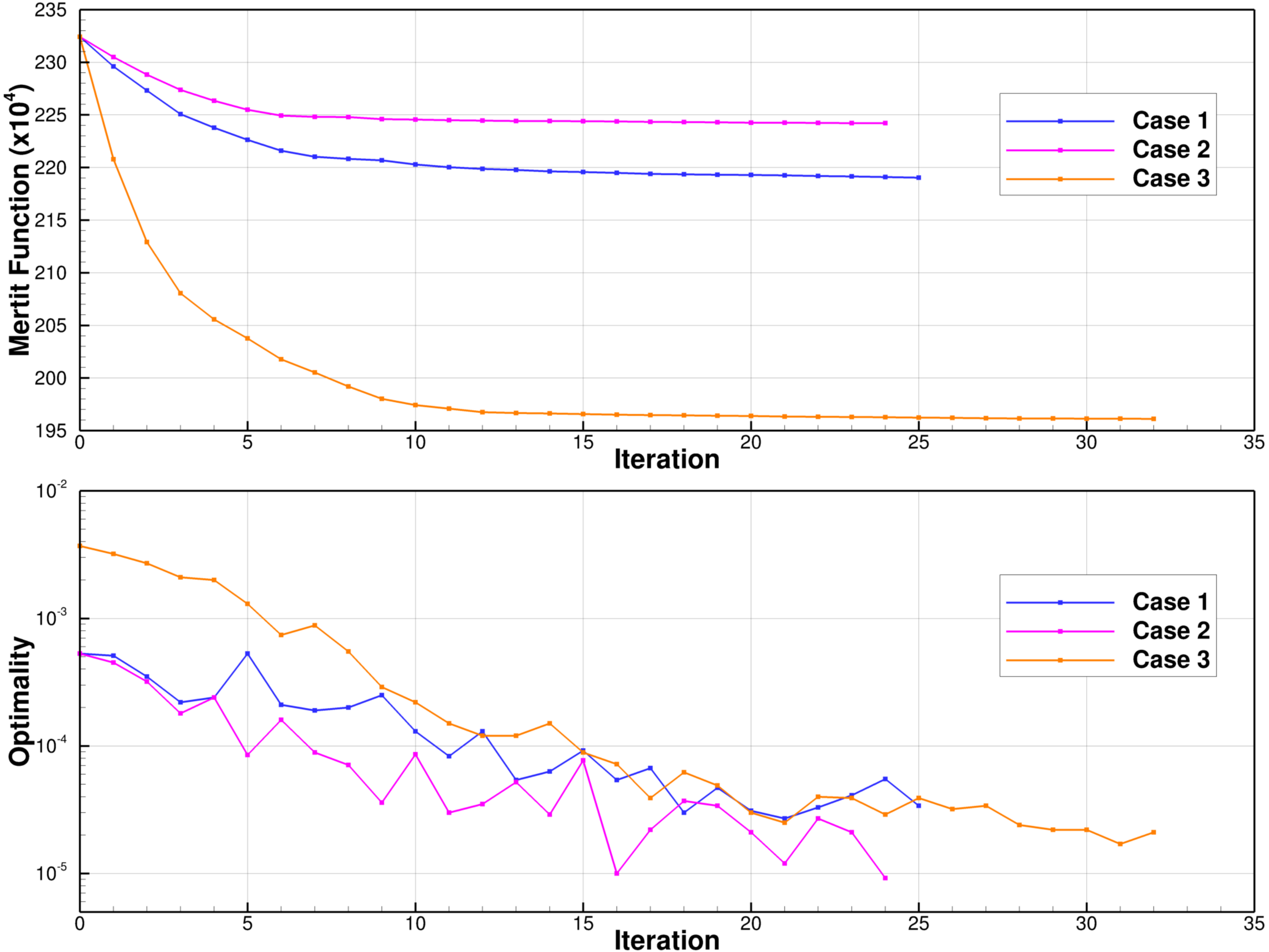

Grid Convergence Study

- Optimized L1 shape analyzed using finer meshes

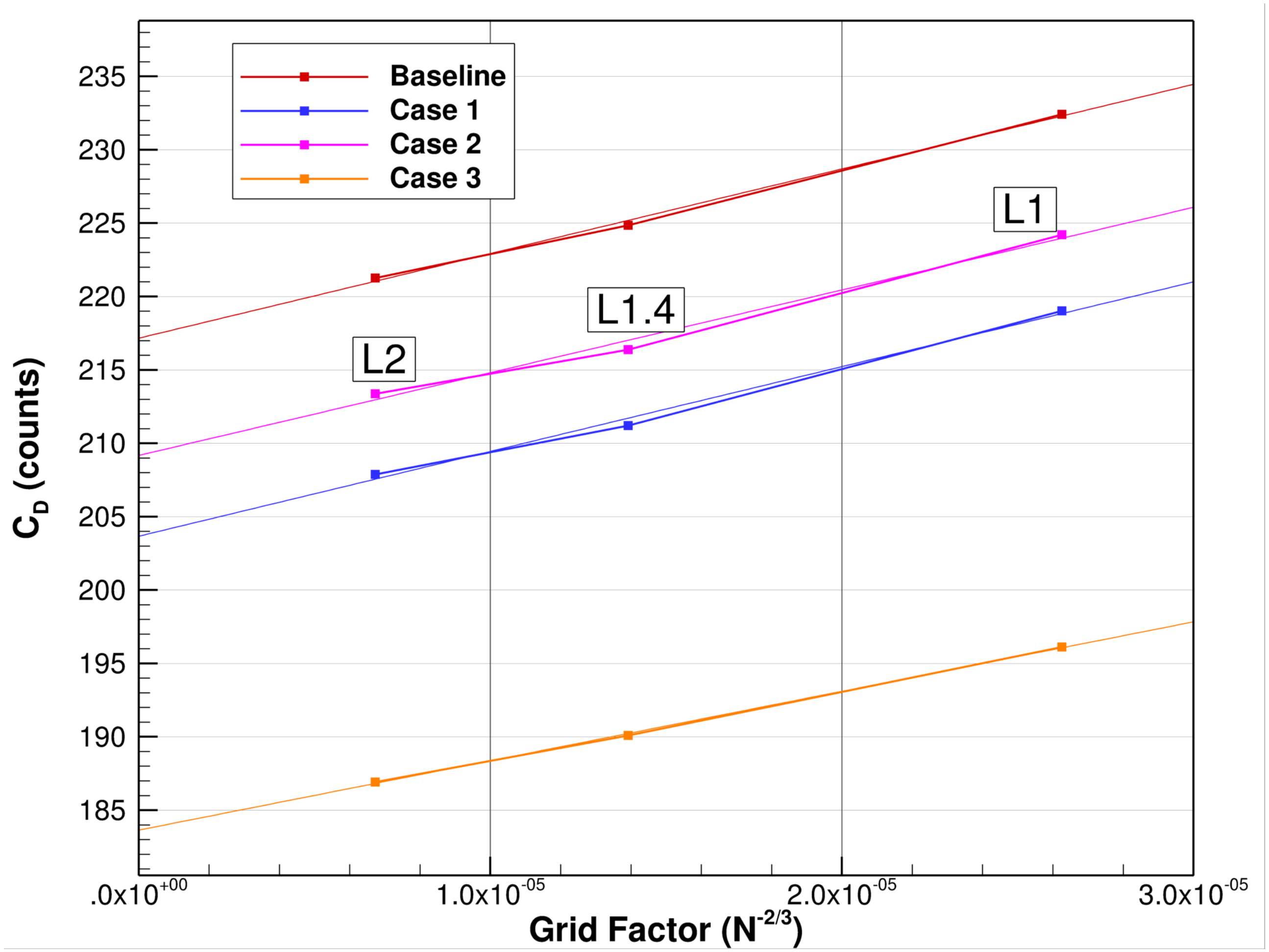

Grid Convergence Study

- Nearly constant drag deltas
- L1 mesh capturing the critical flow features

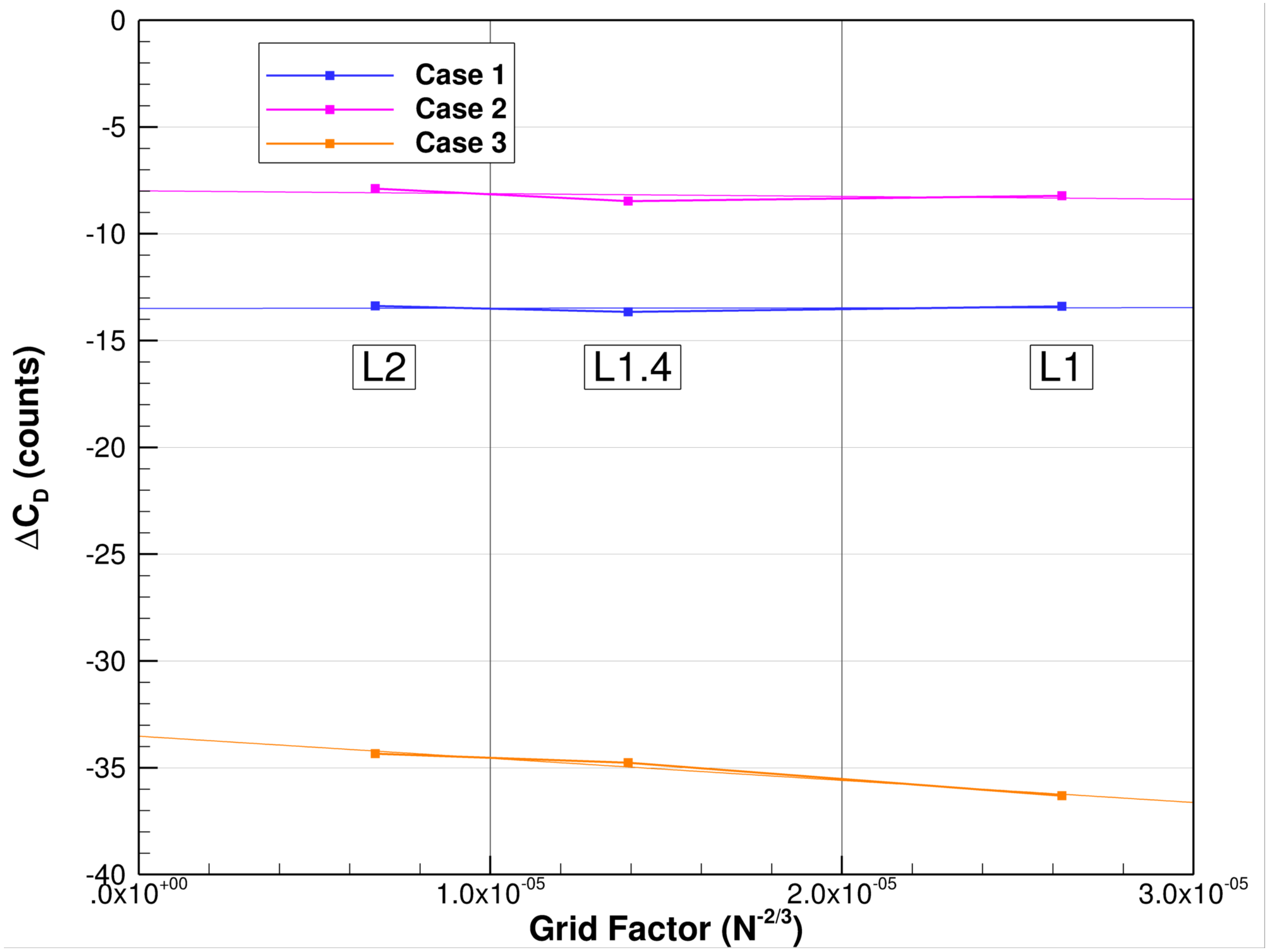

2D Slices of Junction Region

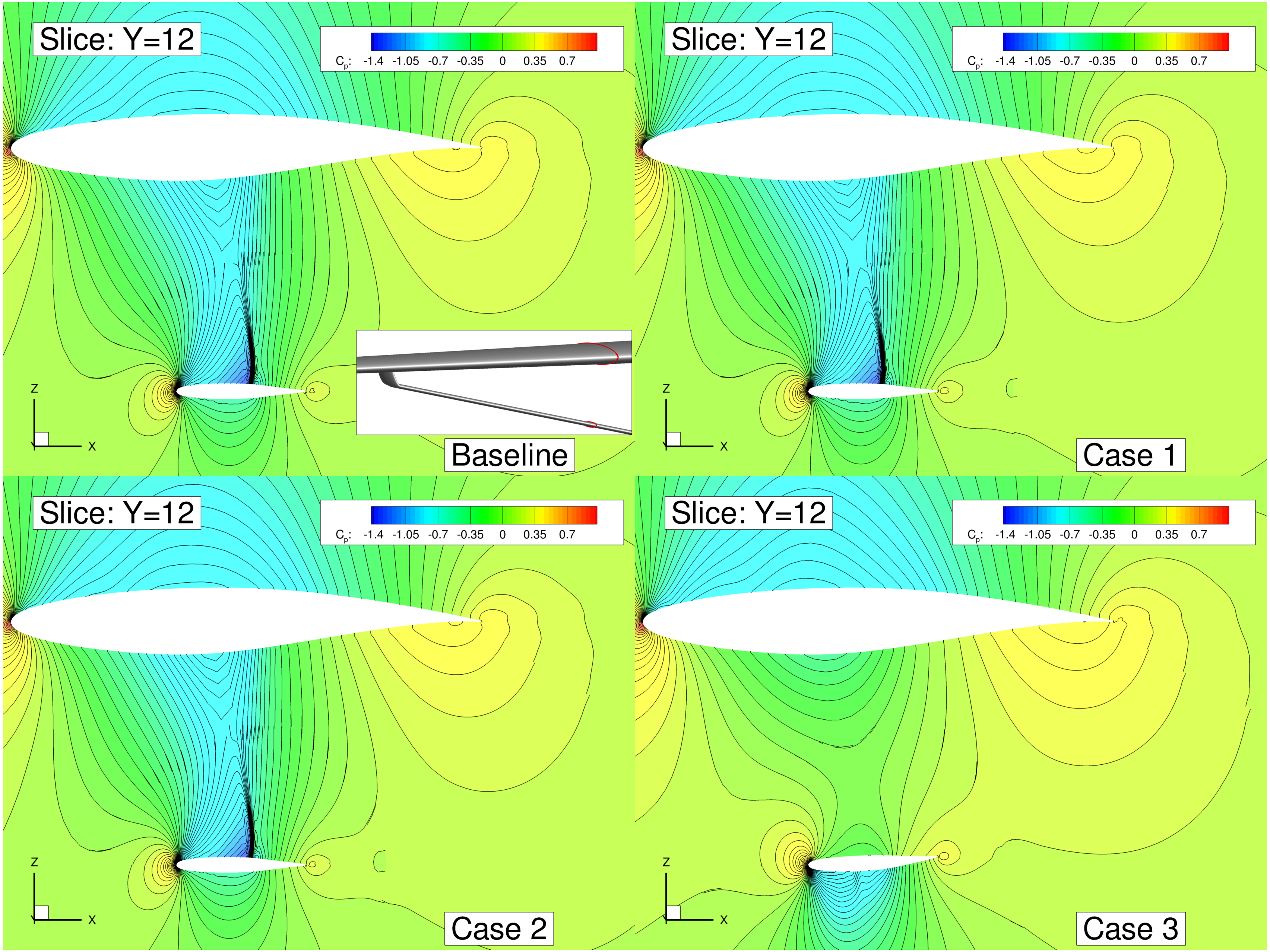

2D Slices of Junction Region

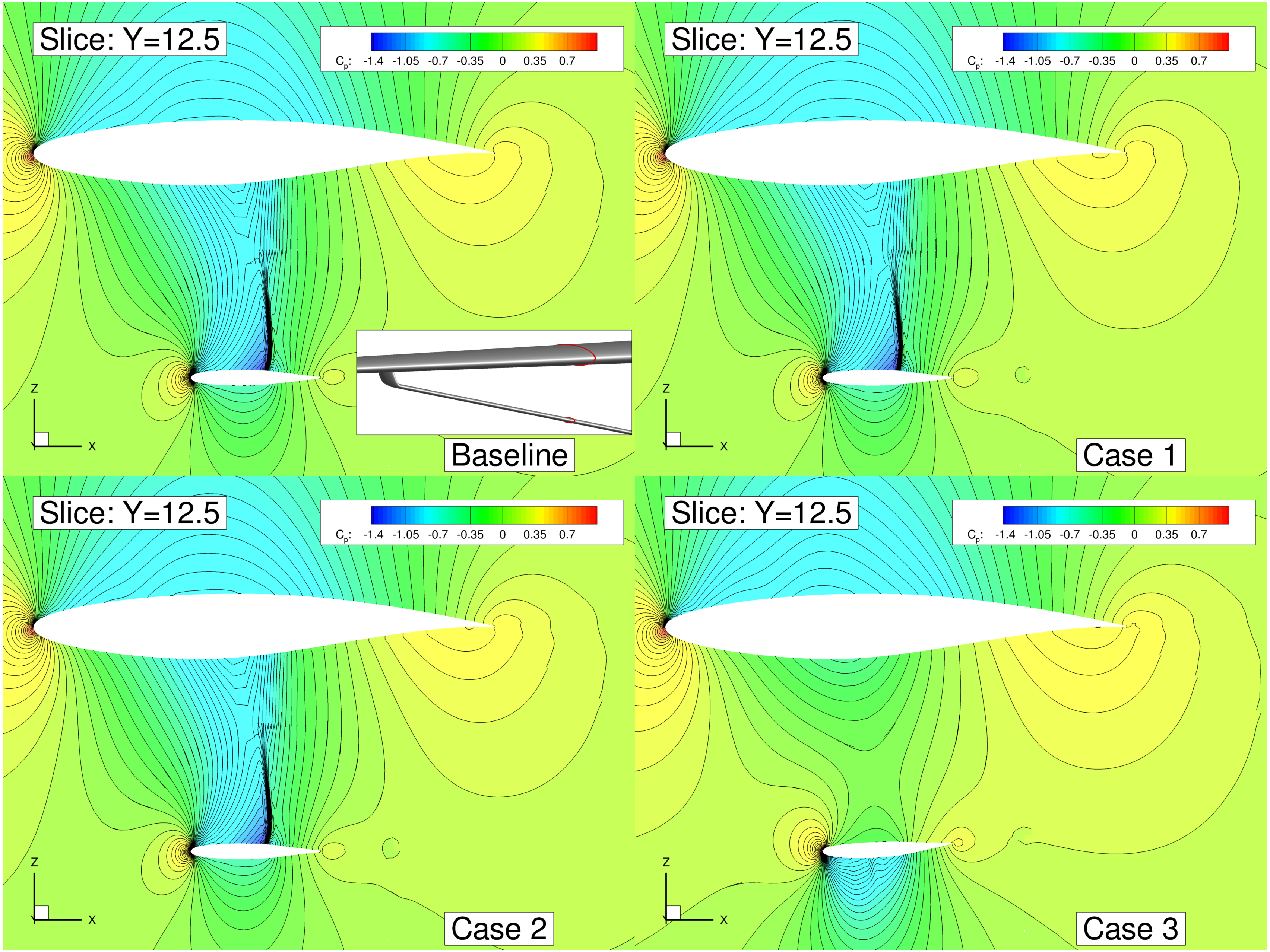

2D Slices of Junction Region

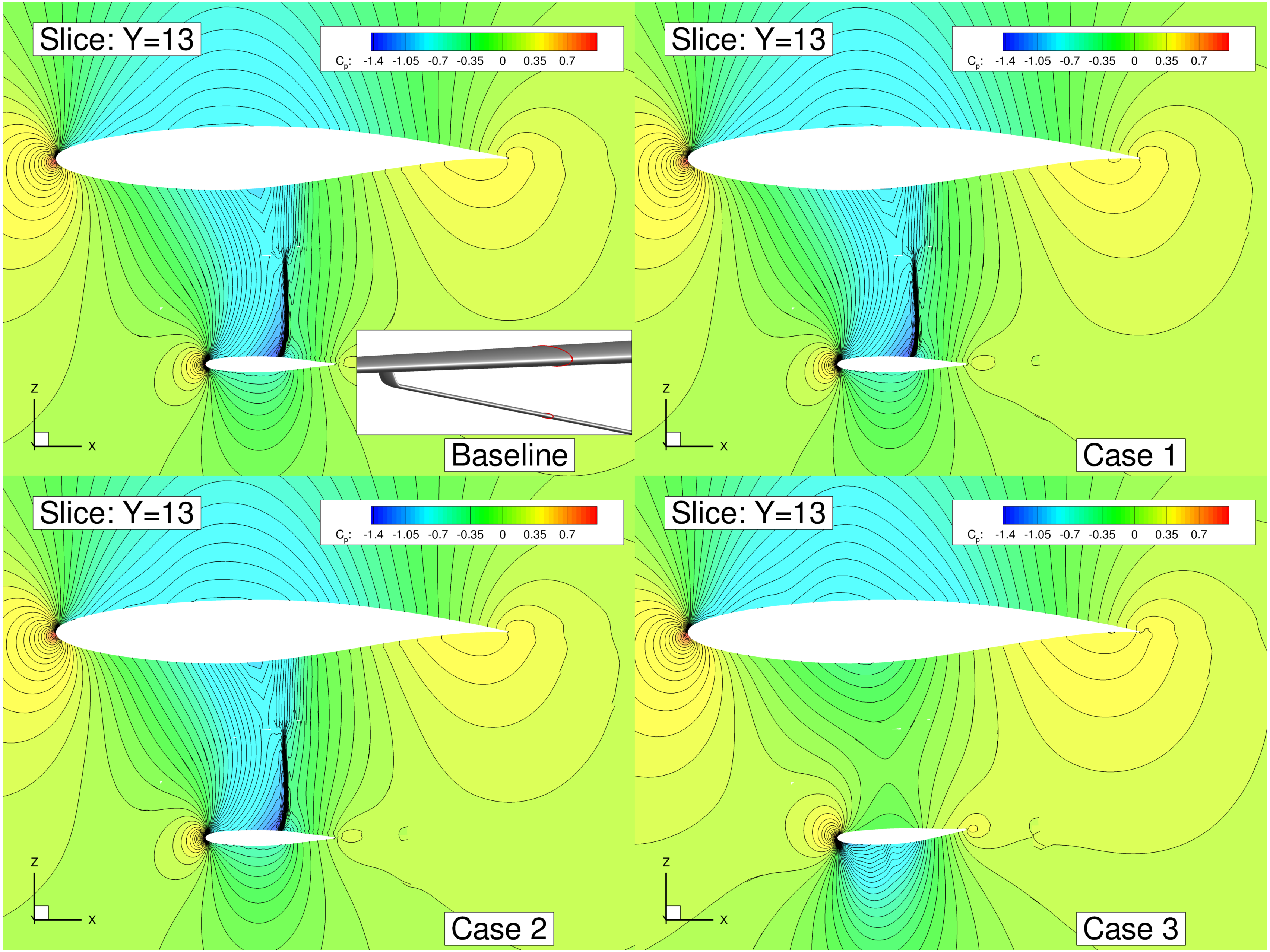

2D Slices of Junction Region

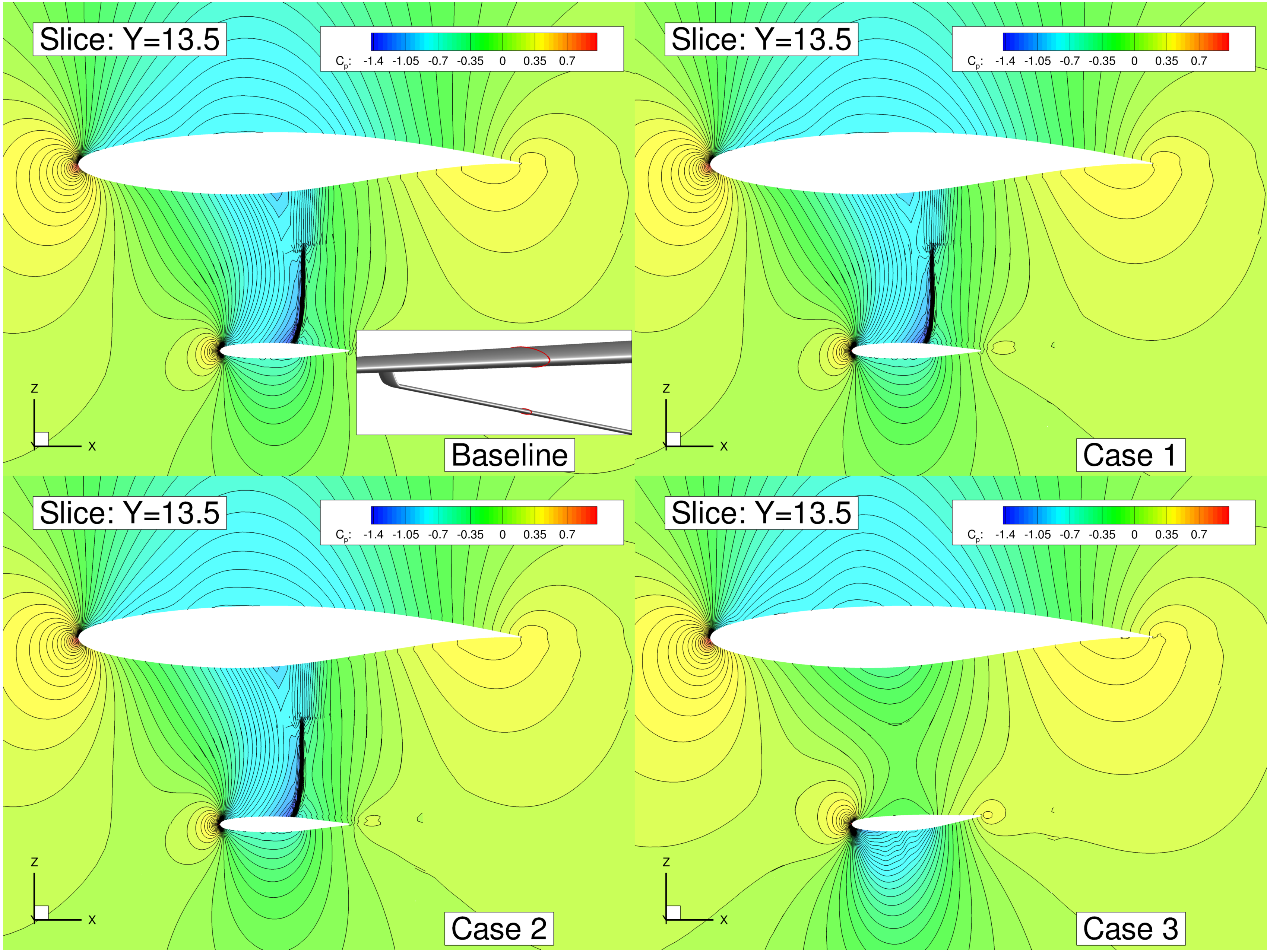

2D Slices of Junction Region

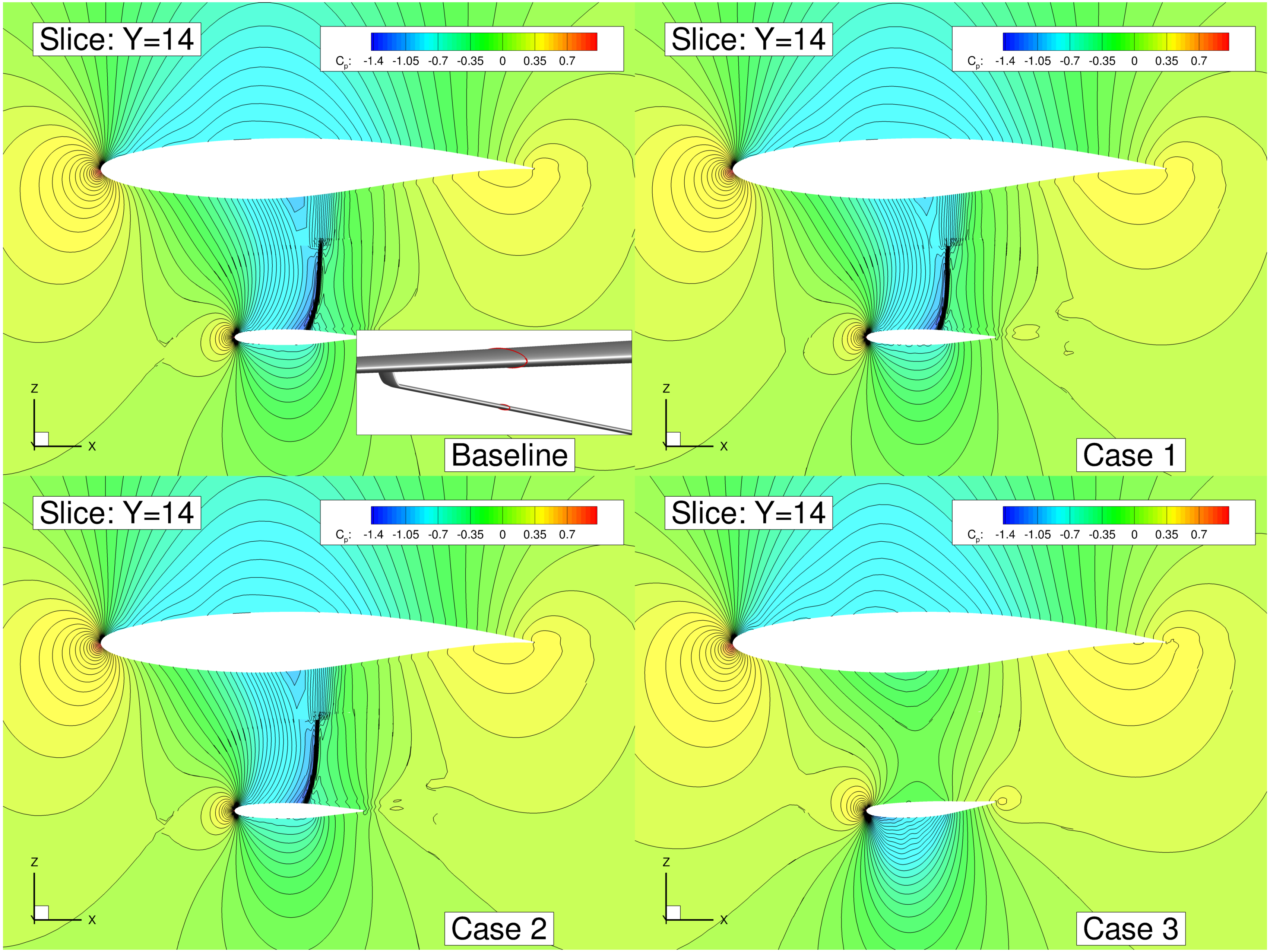

2D Slices of Junction Region

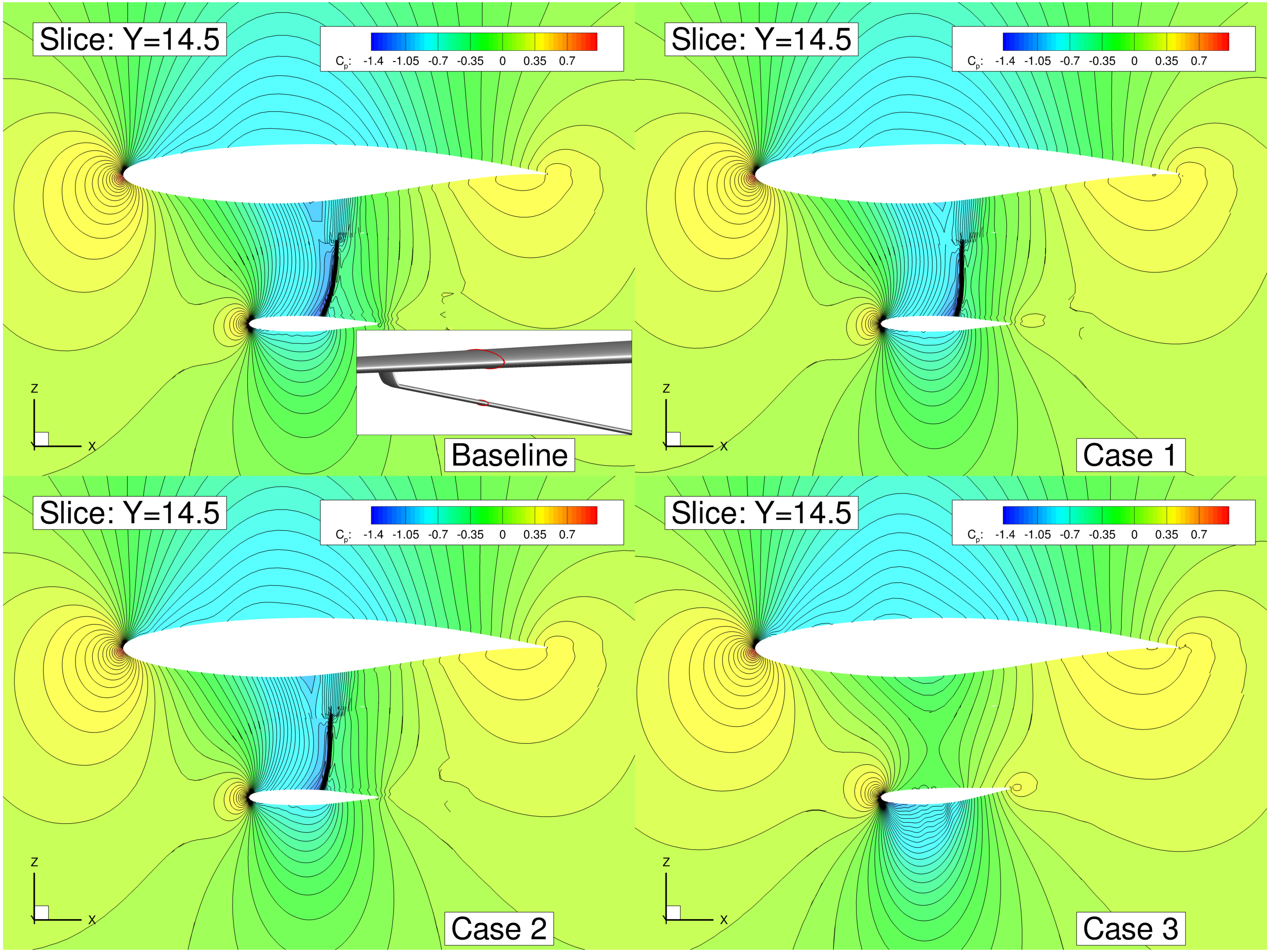

2D Slices of Junction Region

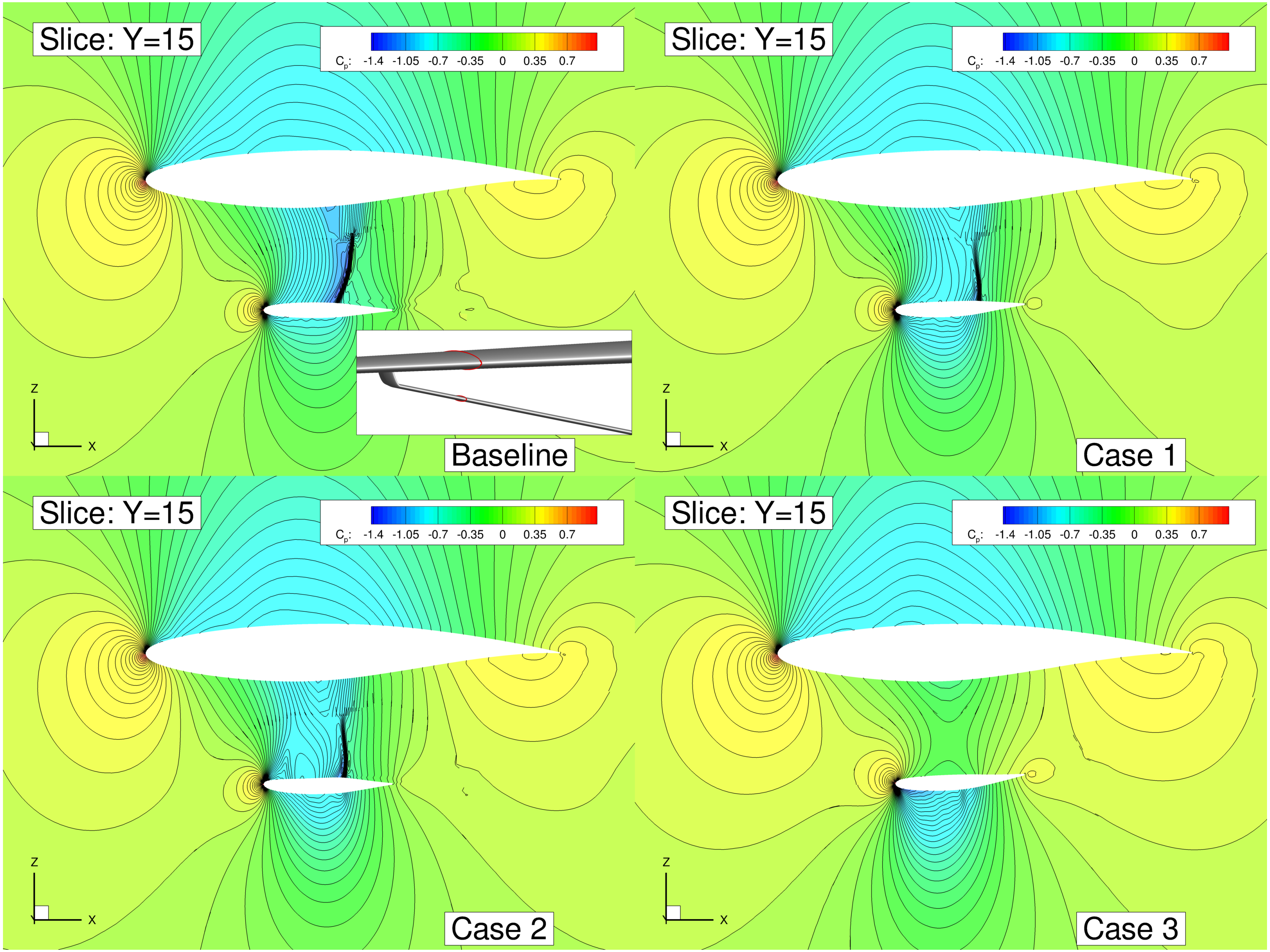

2D Slices of Junction Region

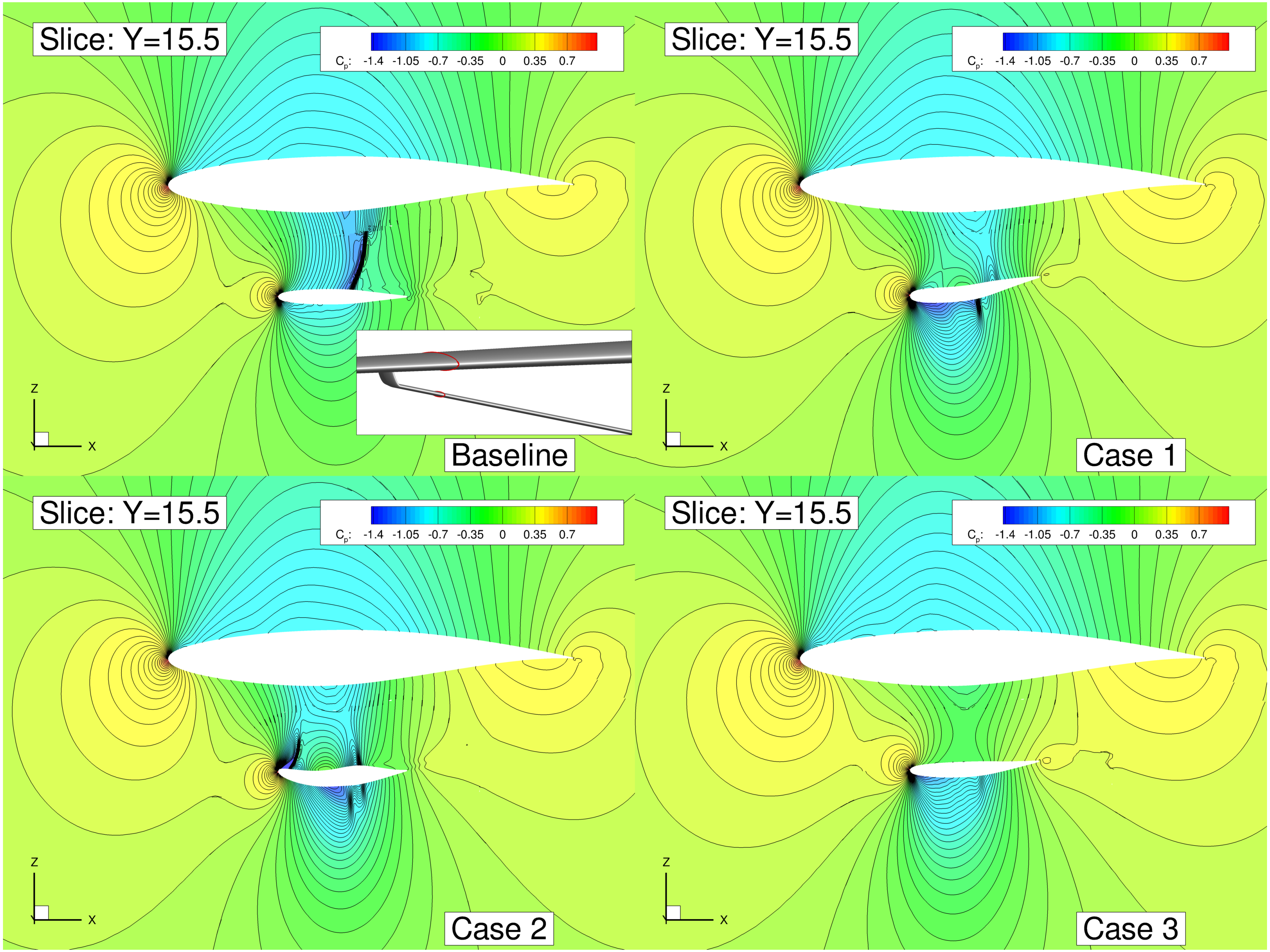

2D Slices of Junction Region

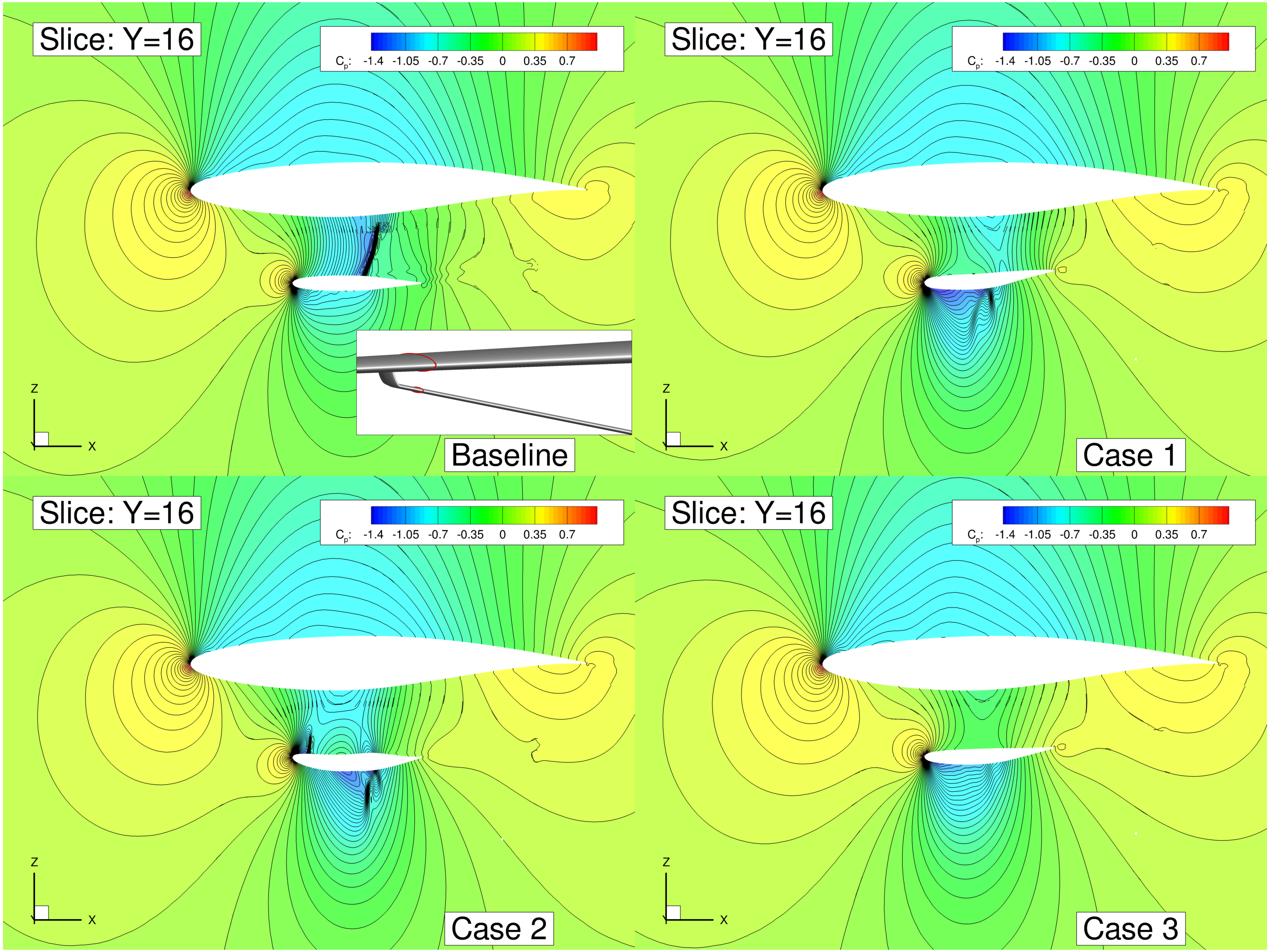

2D Slices of Junction Region

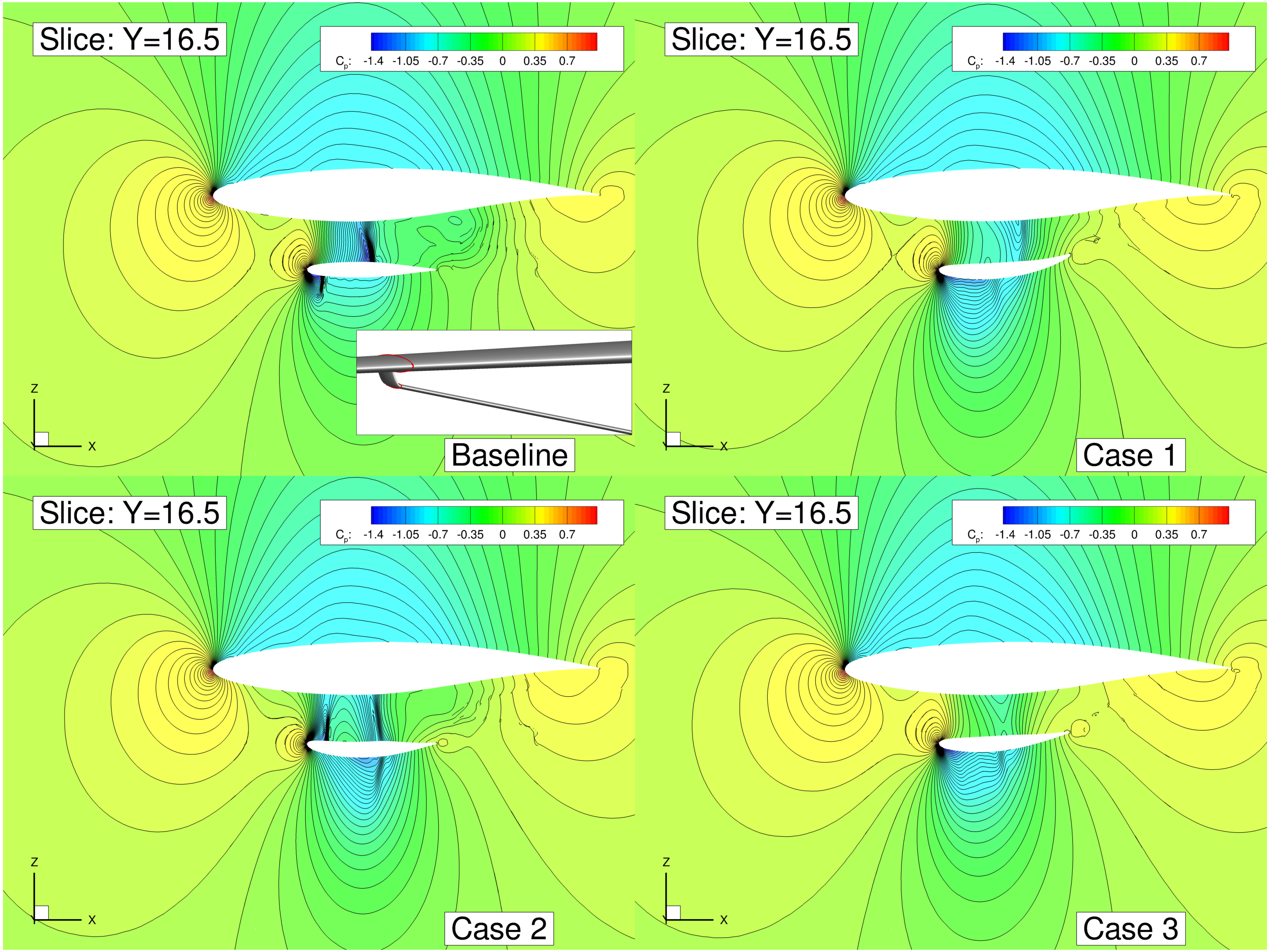

2D Slices of Junction Region

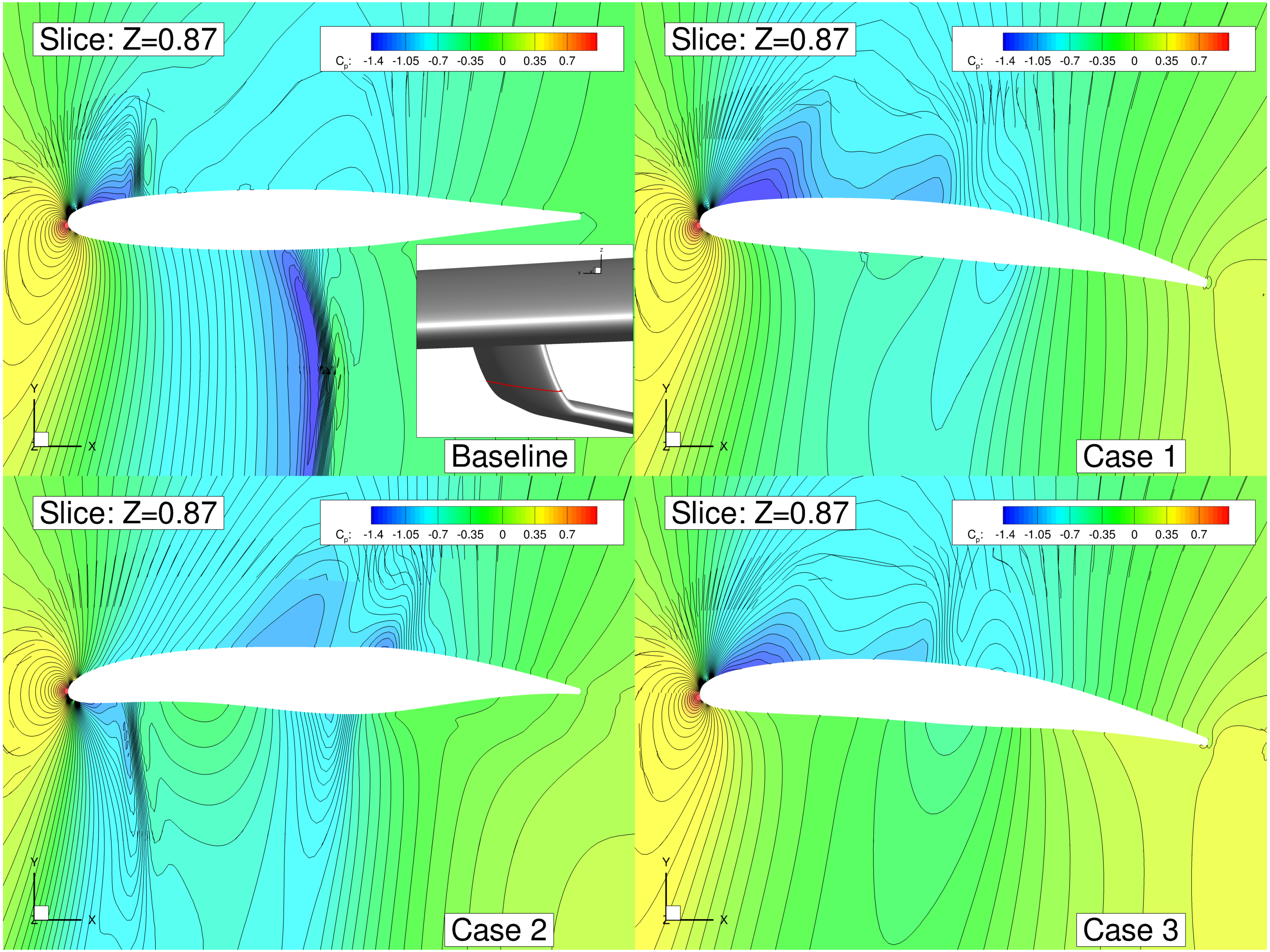

2D Slices of Junction Region

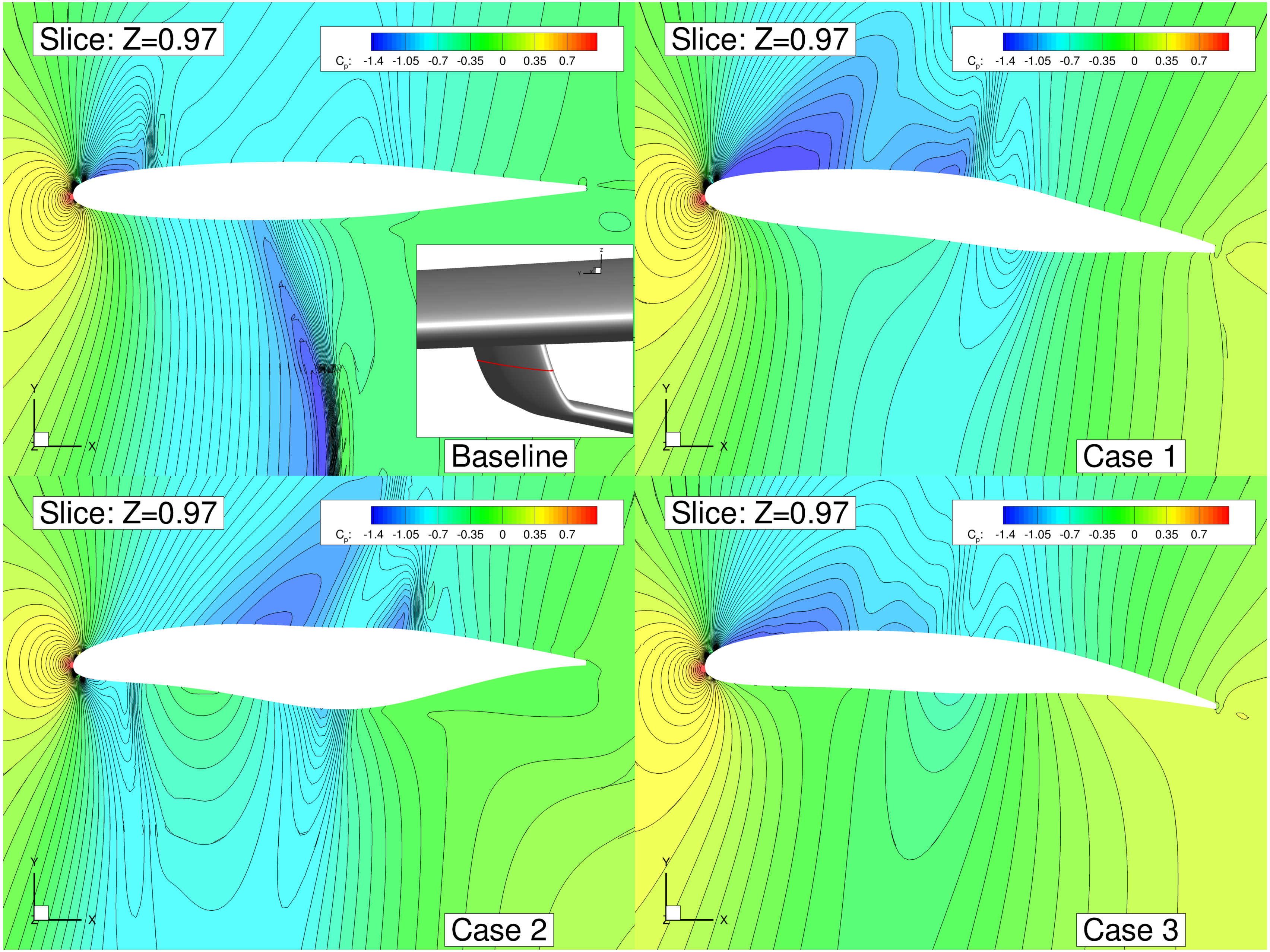

2D Slices of Junction Region

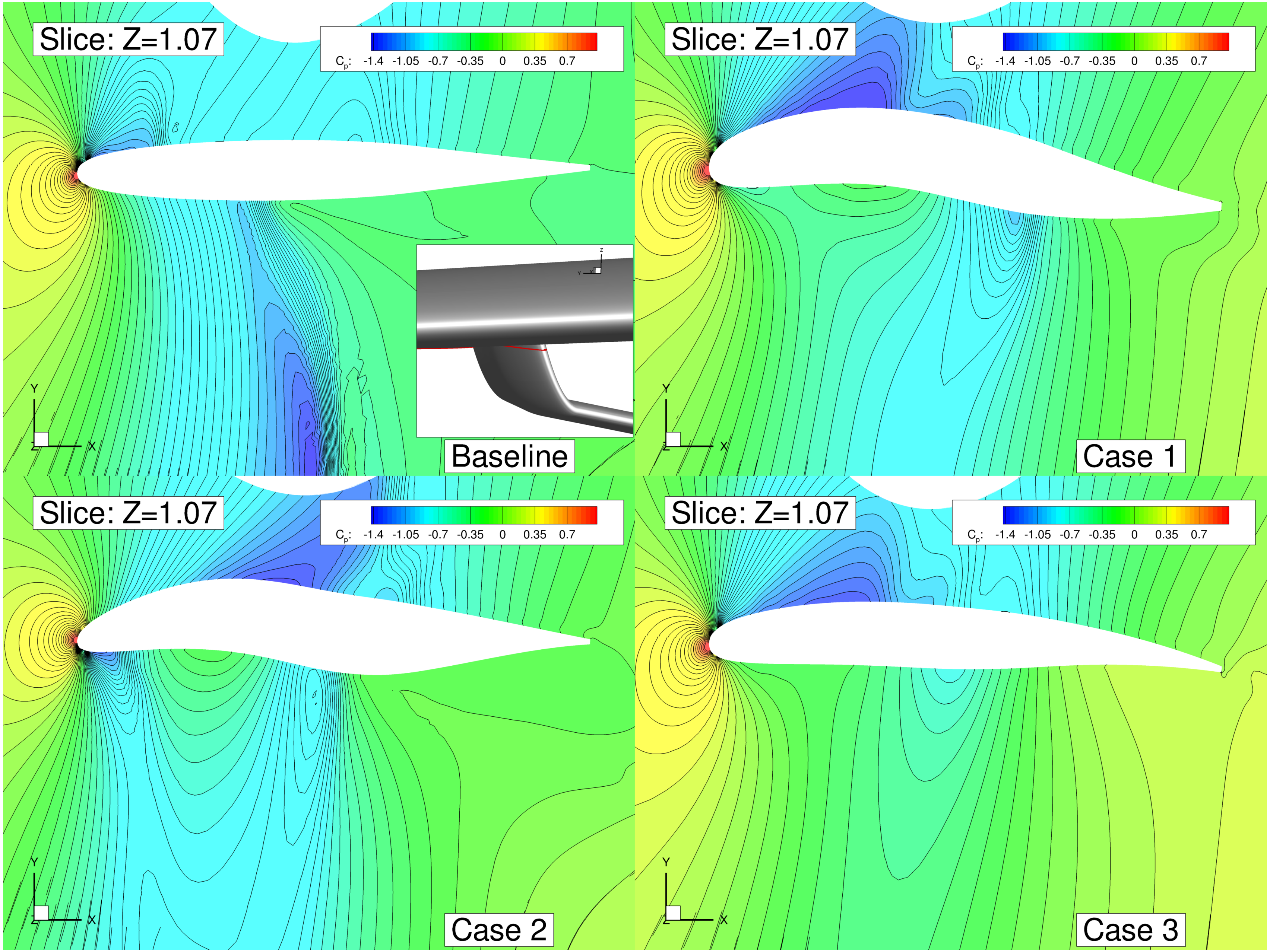

2D Slices of Junction Region

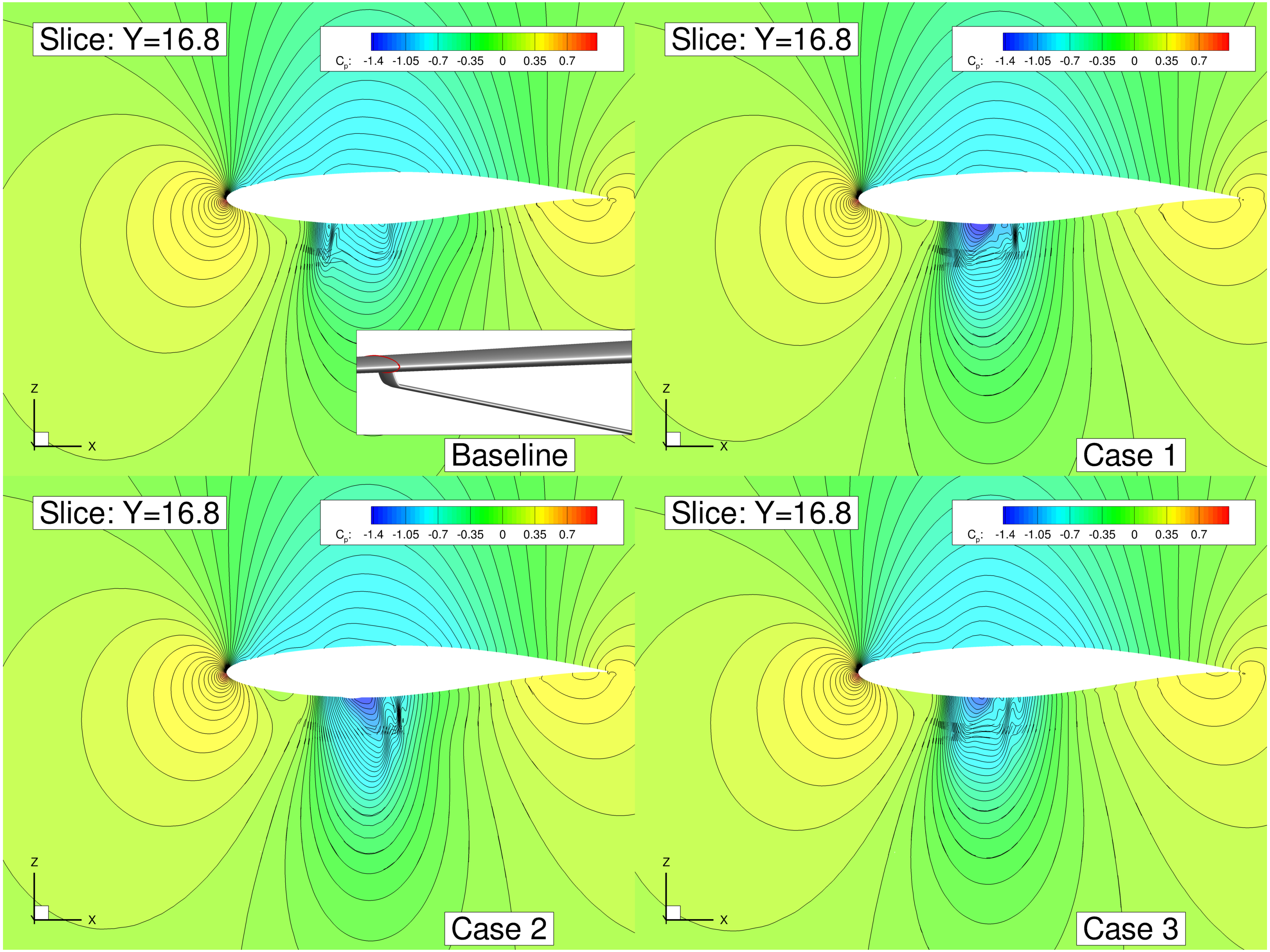

2D Slices of Junction Region

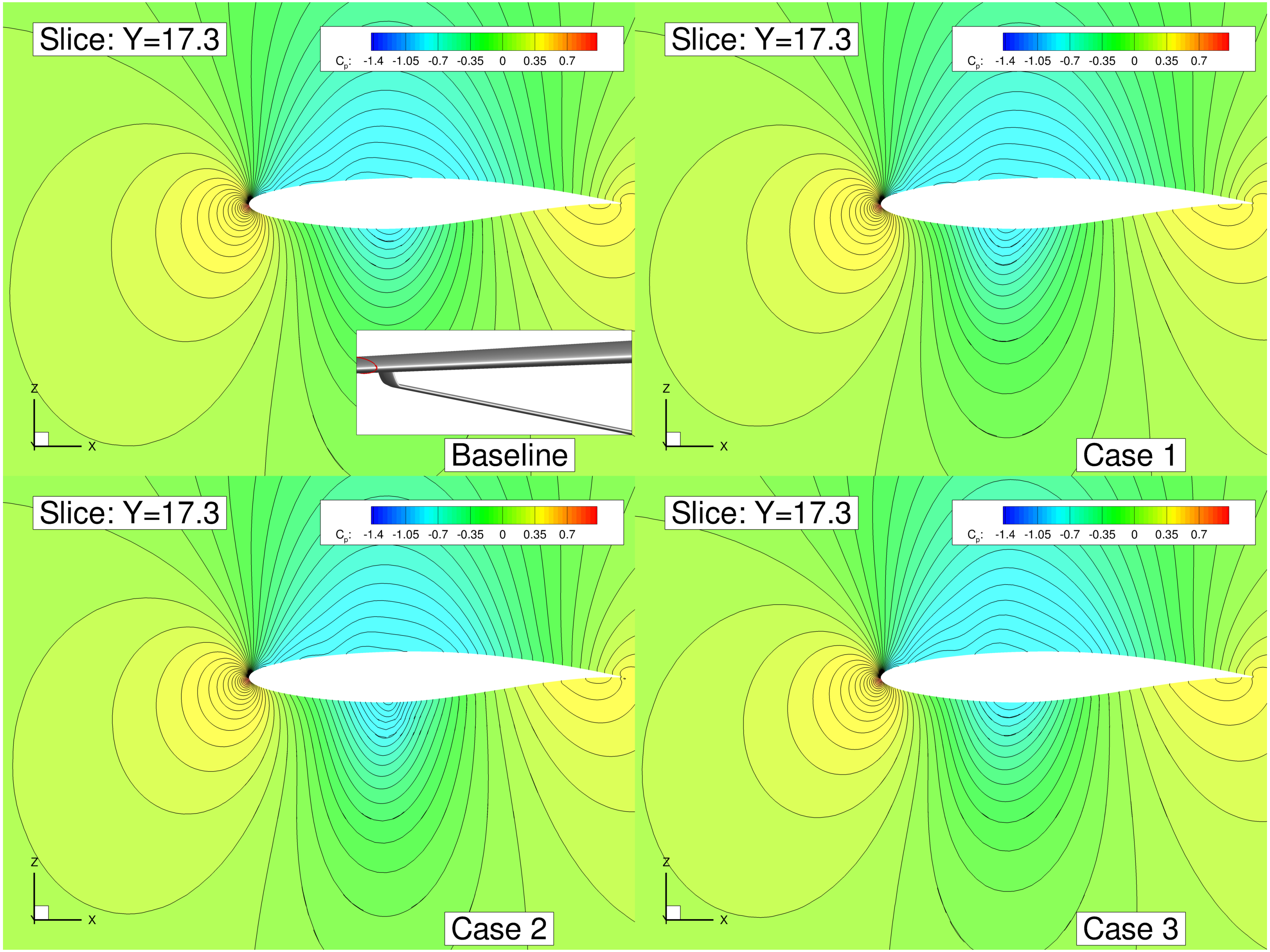

2D Slices of Junction Region

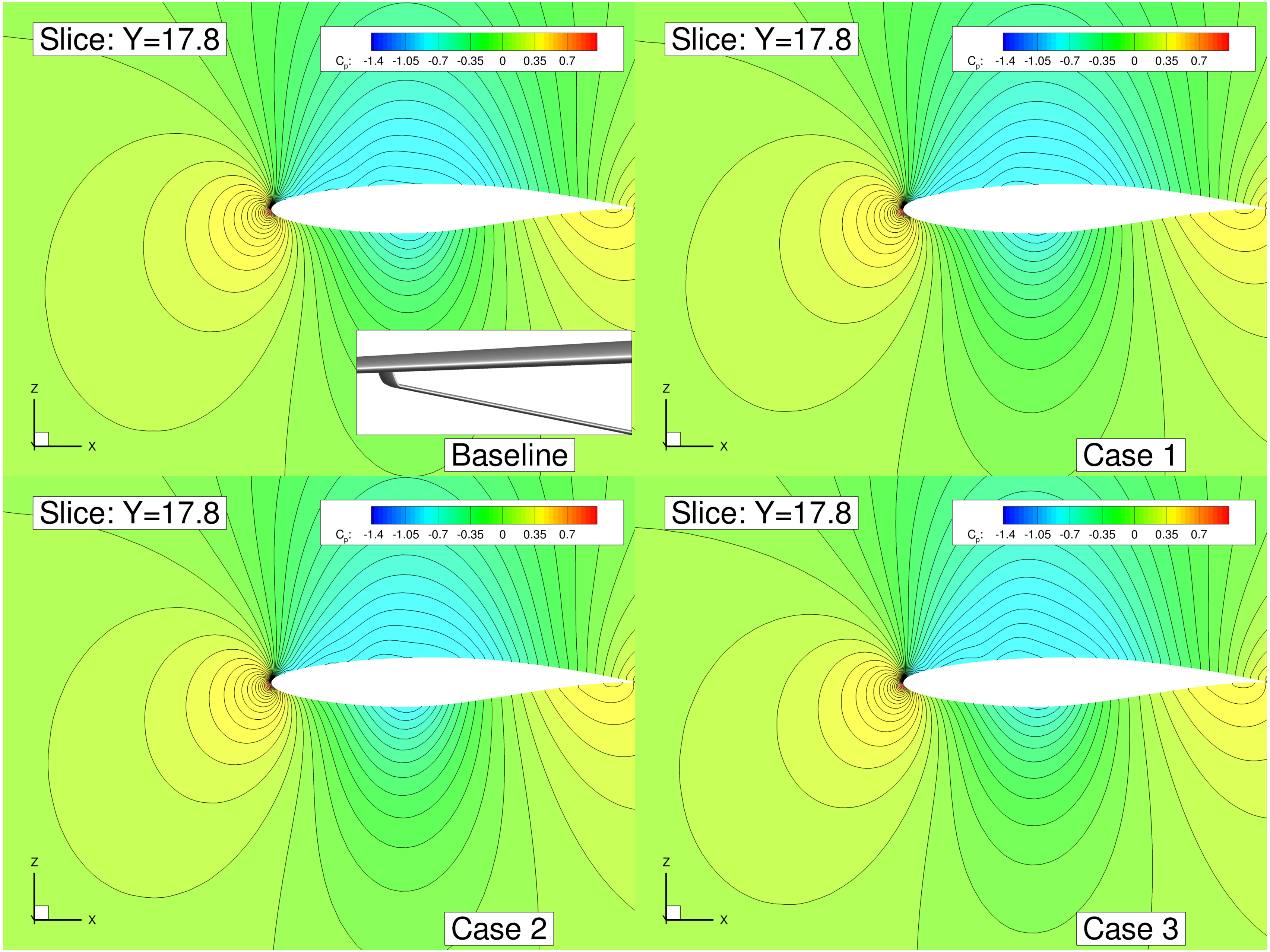

2D Slices of Junction Region

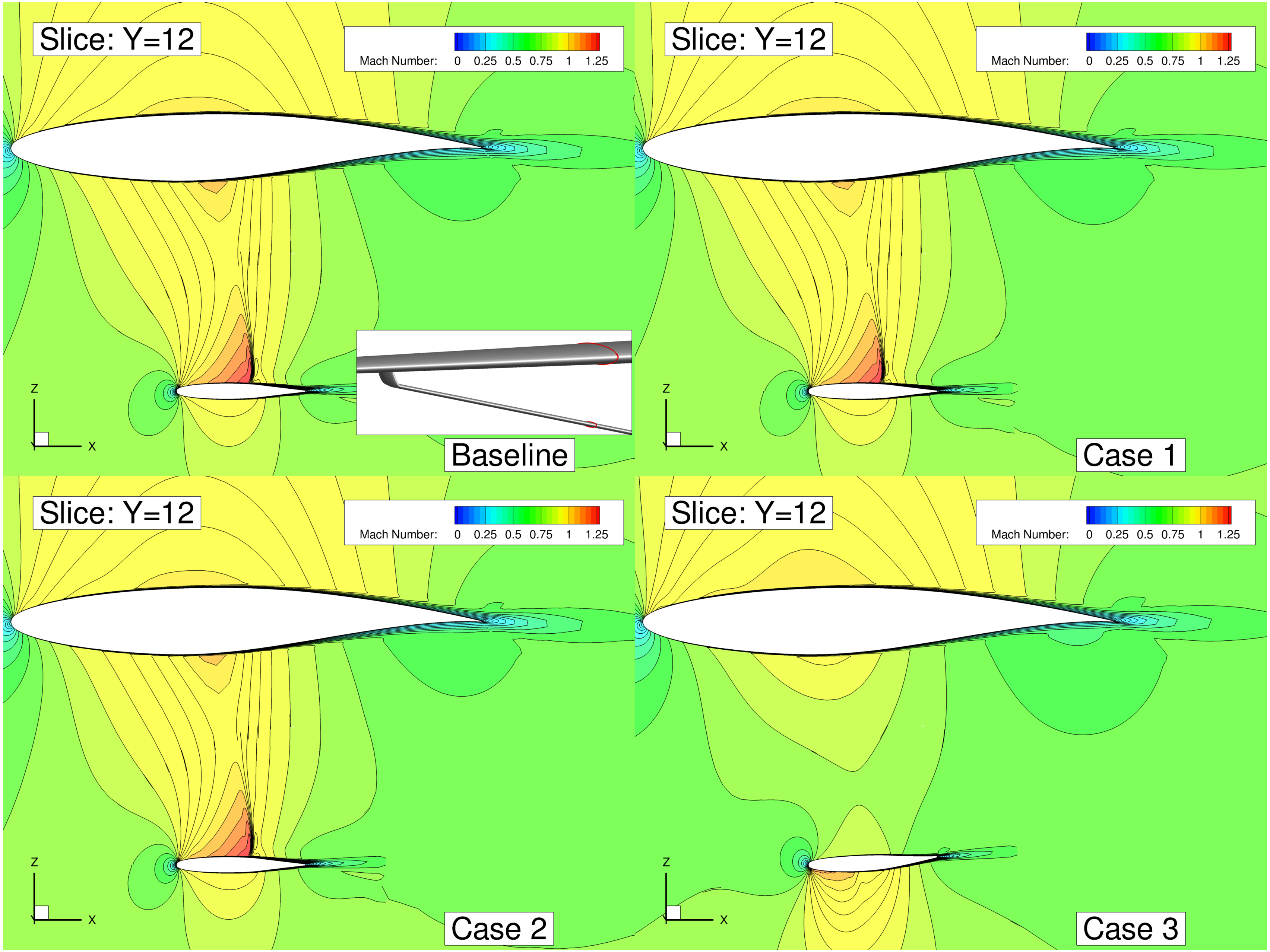

2D Slices of Junction Region

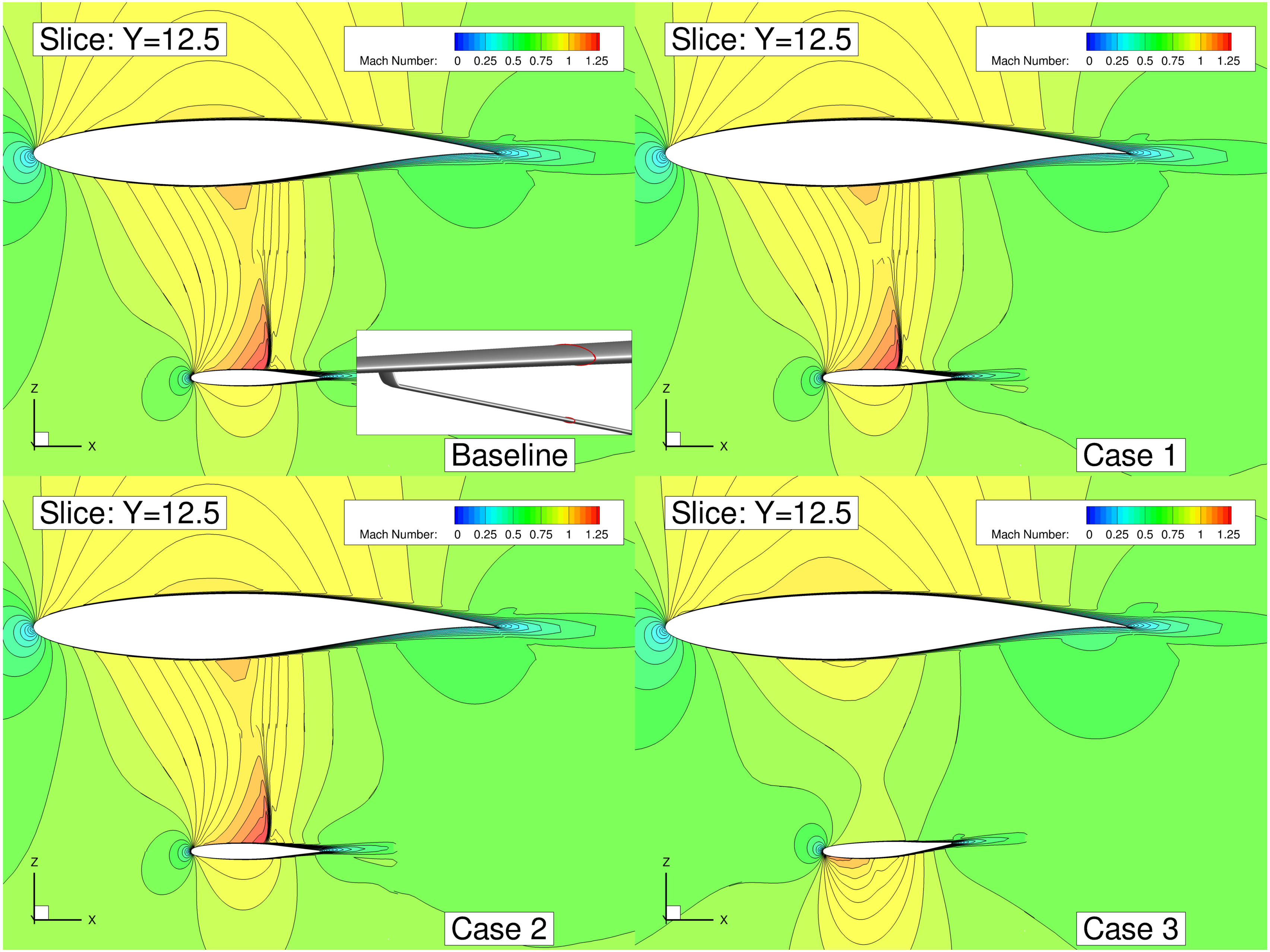

2D Slices of Junction Region

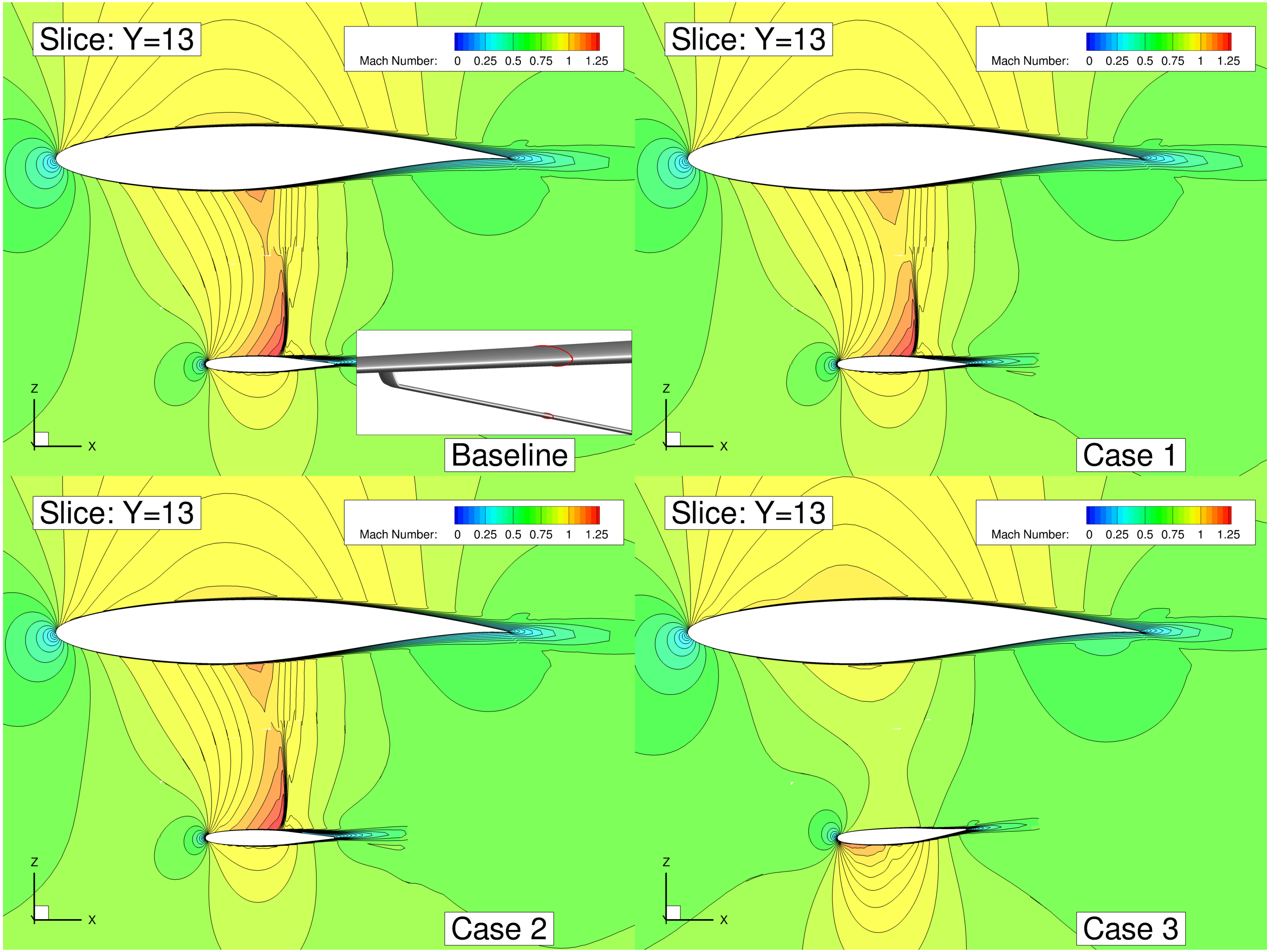

2D Slices of Junction Region

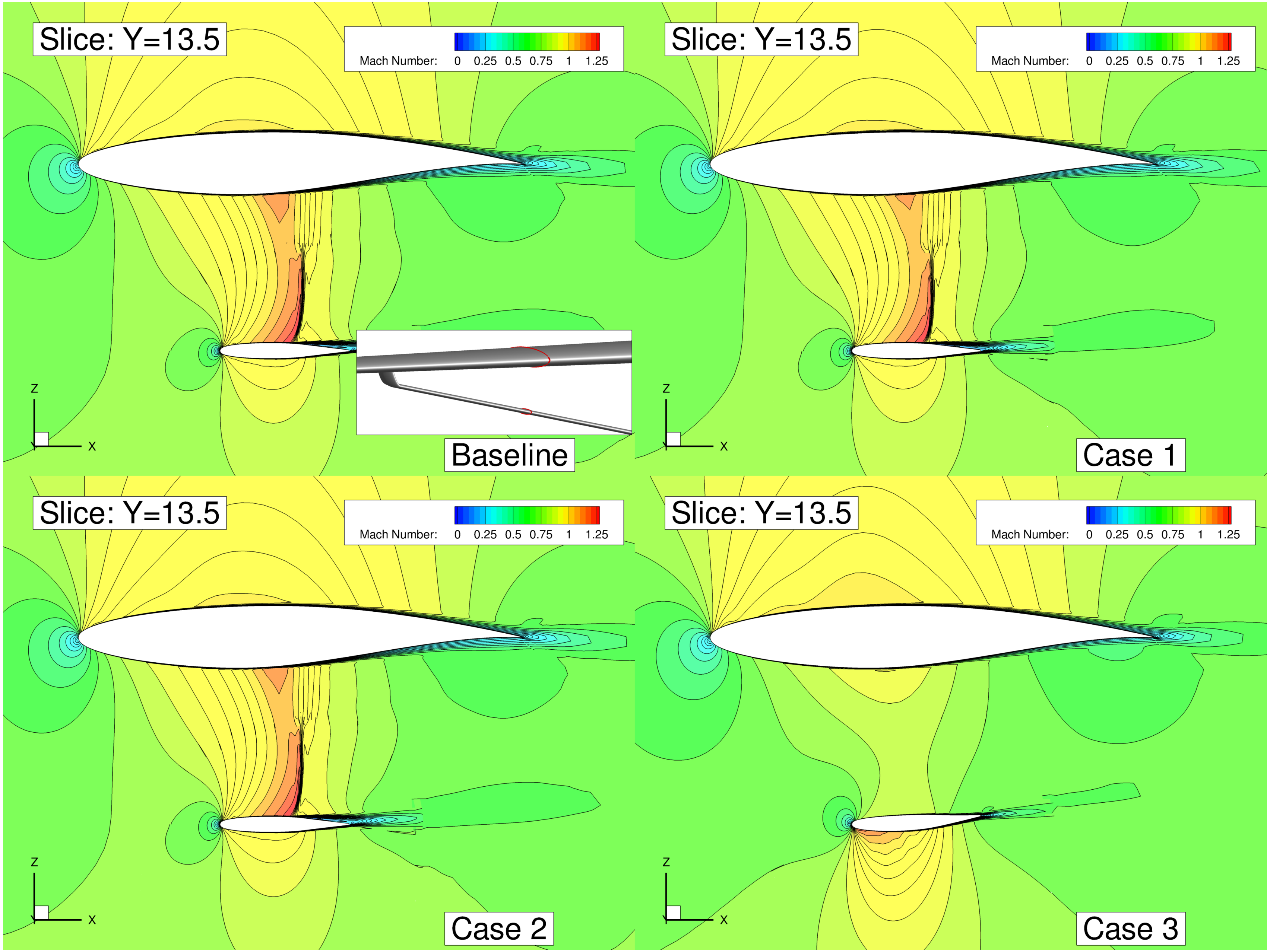

2D Slices of Junction Region

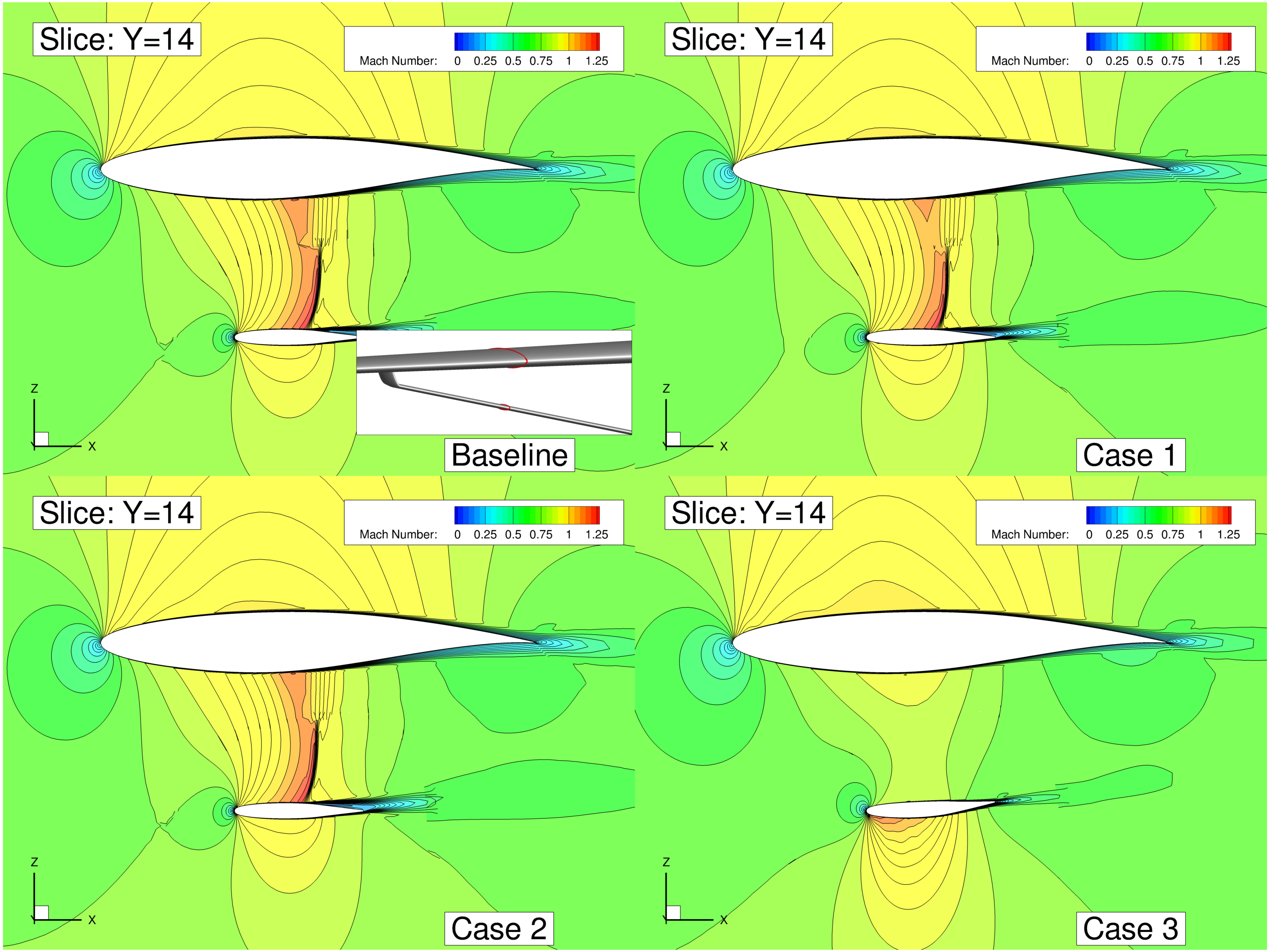

2D Slices of Junction Region

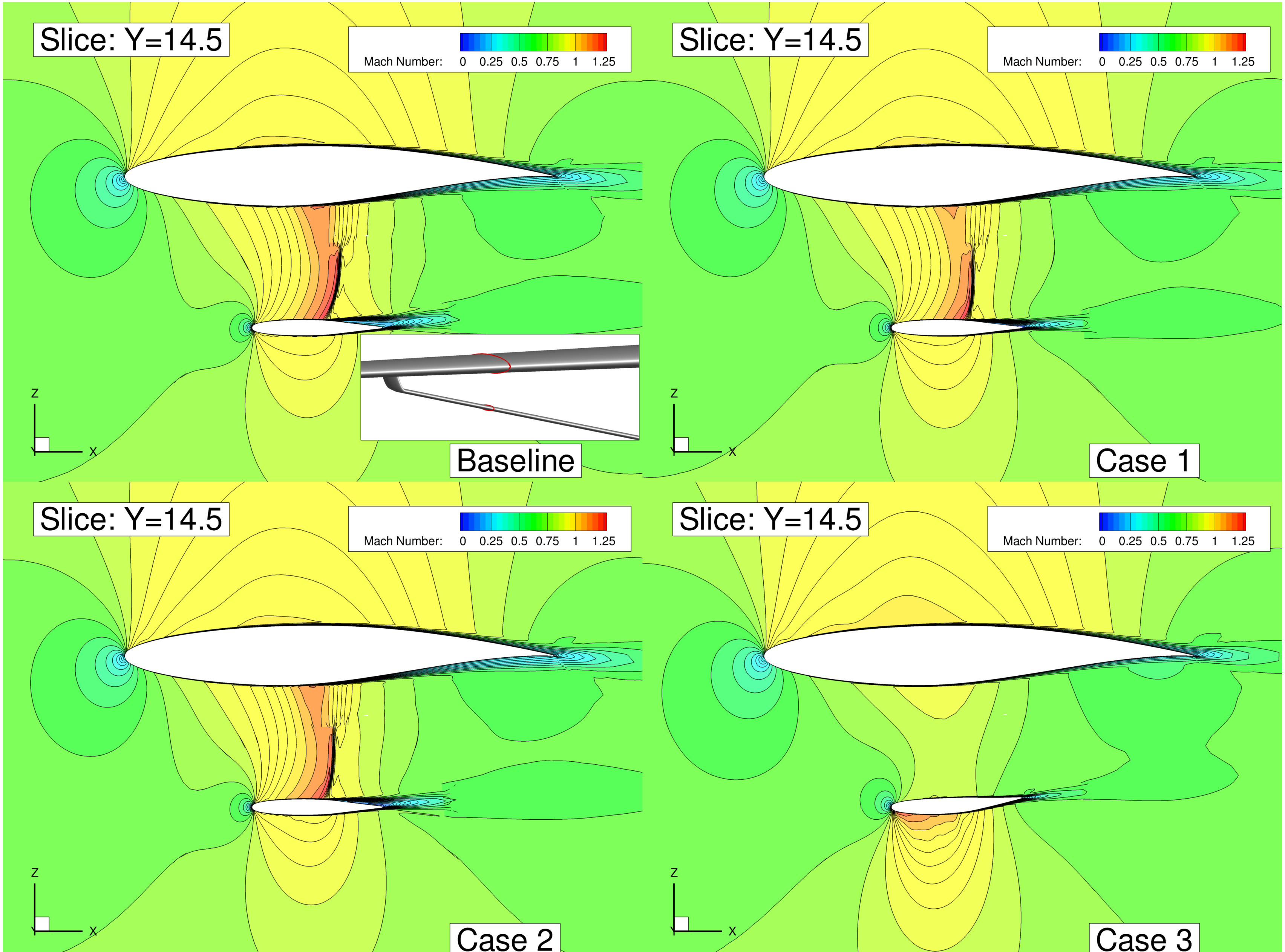

2D Slices of Junction Region

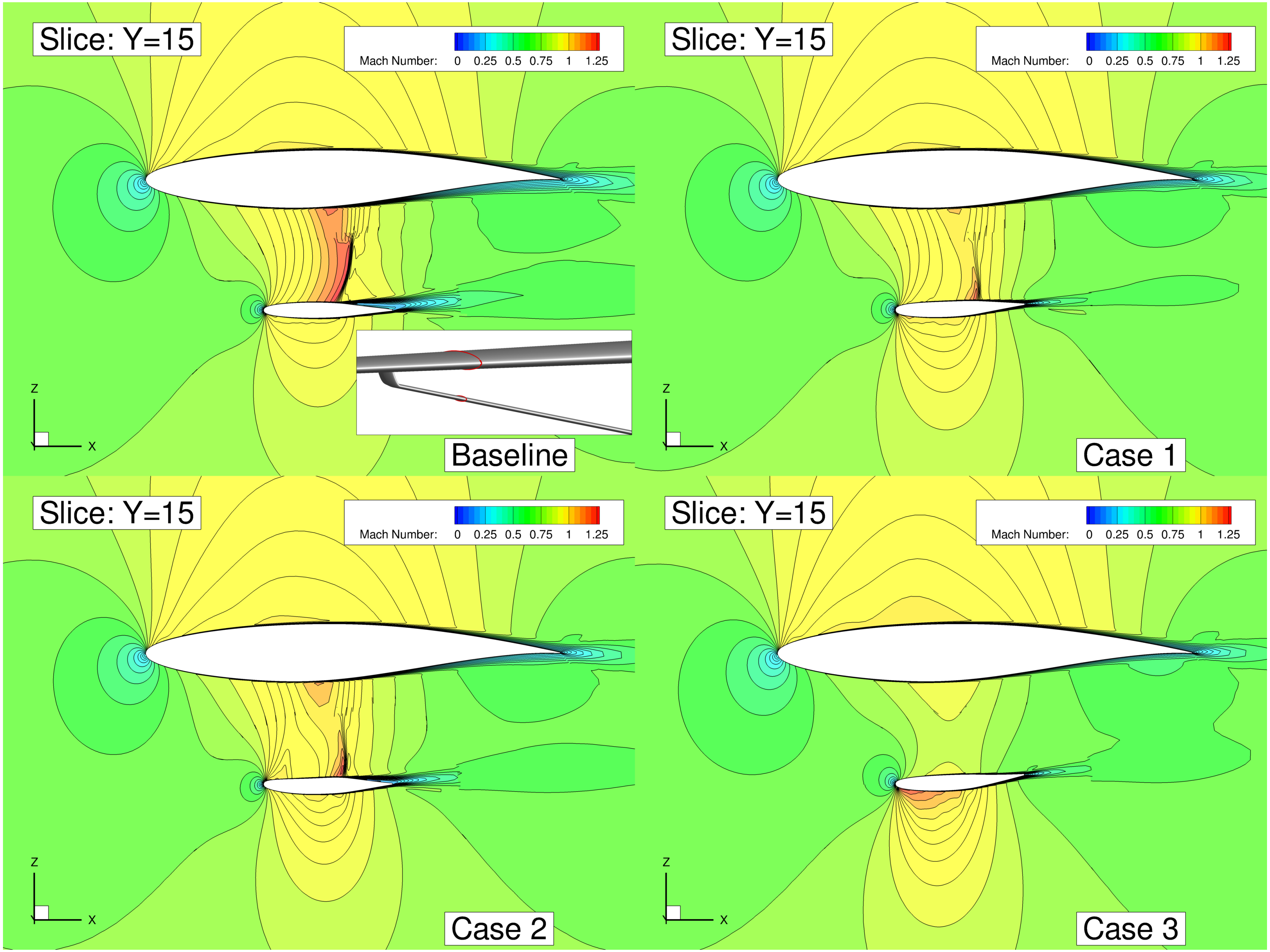

2D Slices of Junction Region

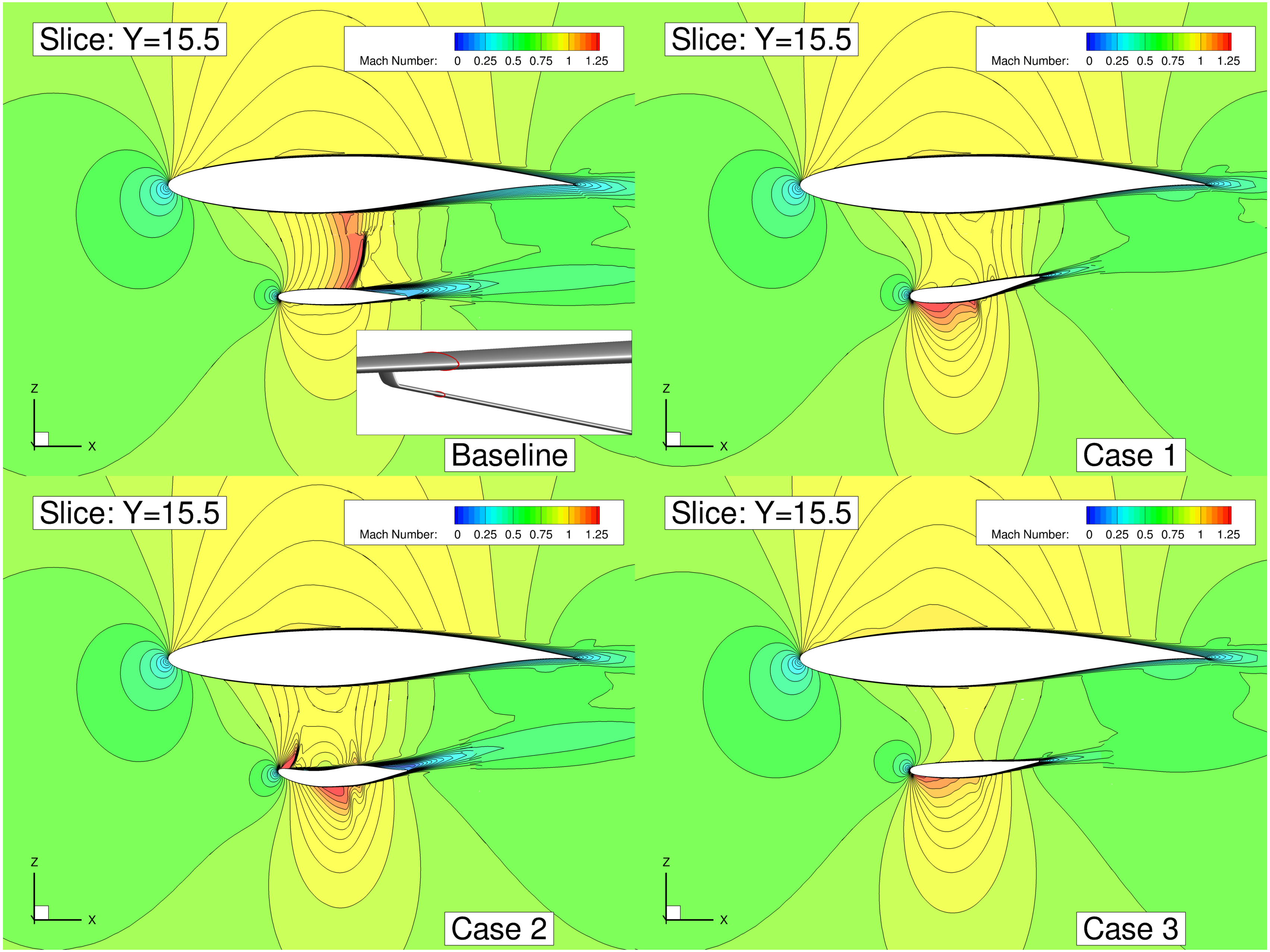

2D Slices of Junction Region

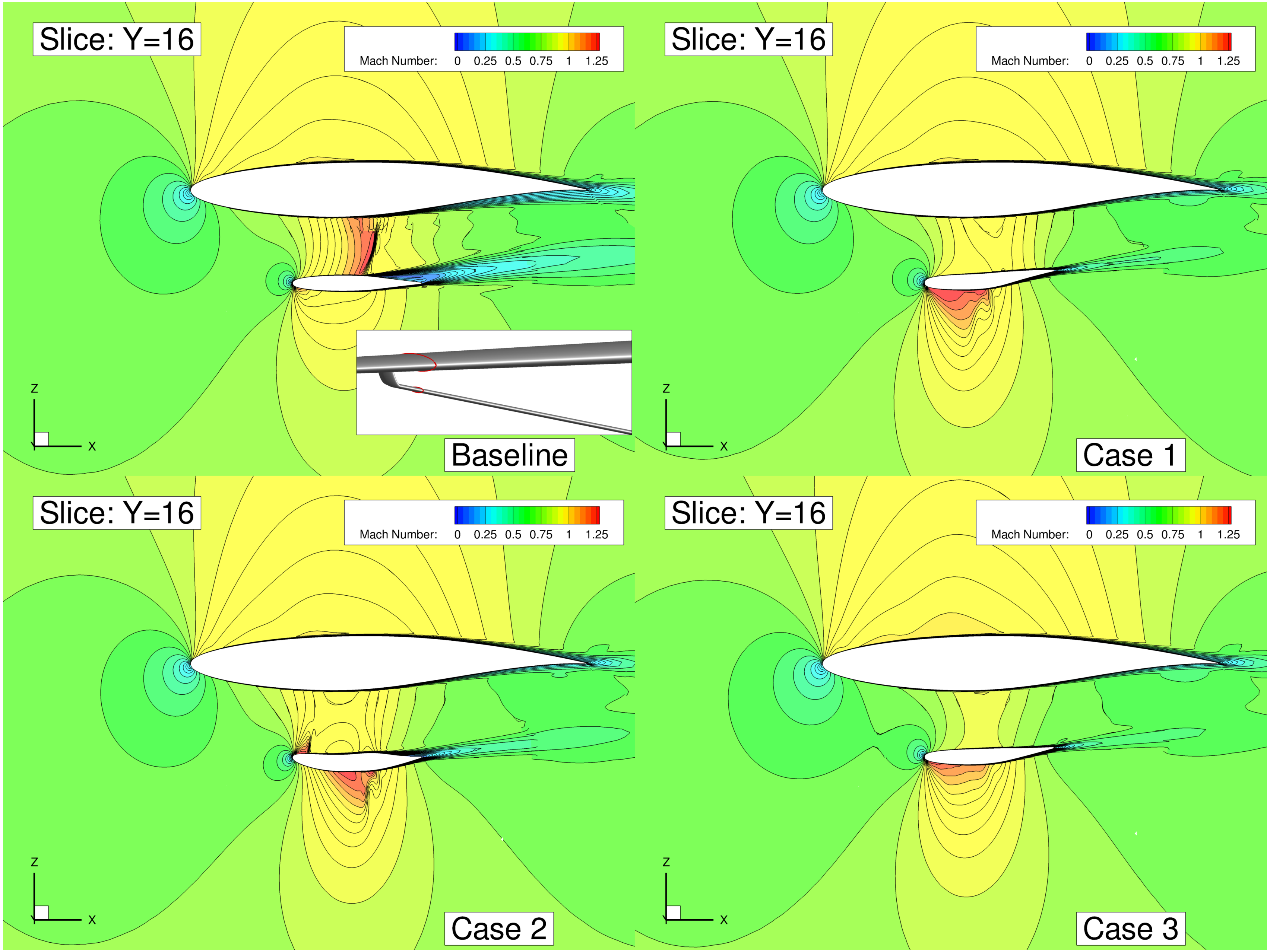

2D Slices of Junction Region

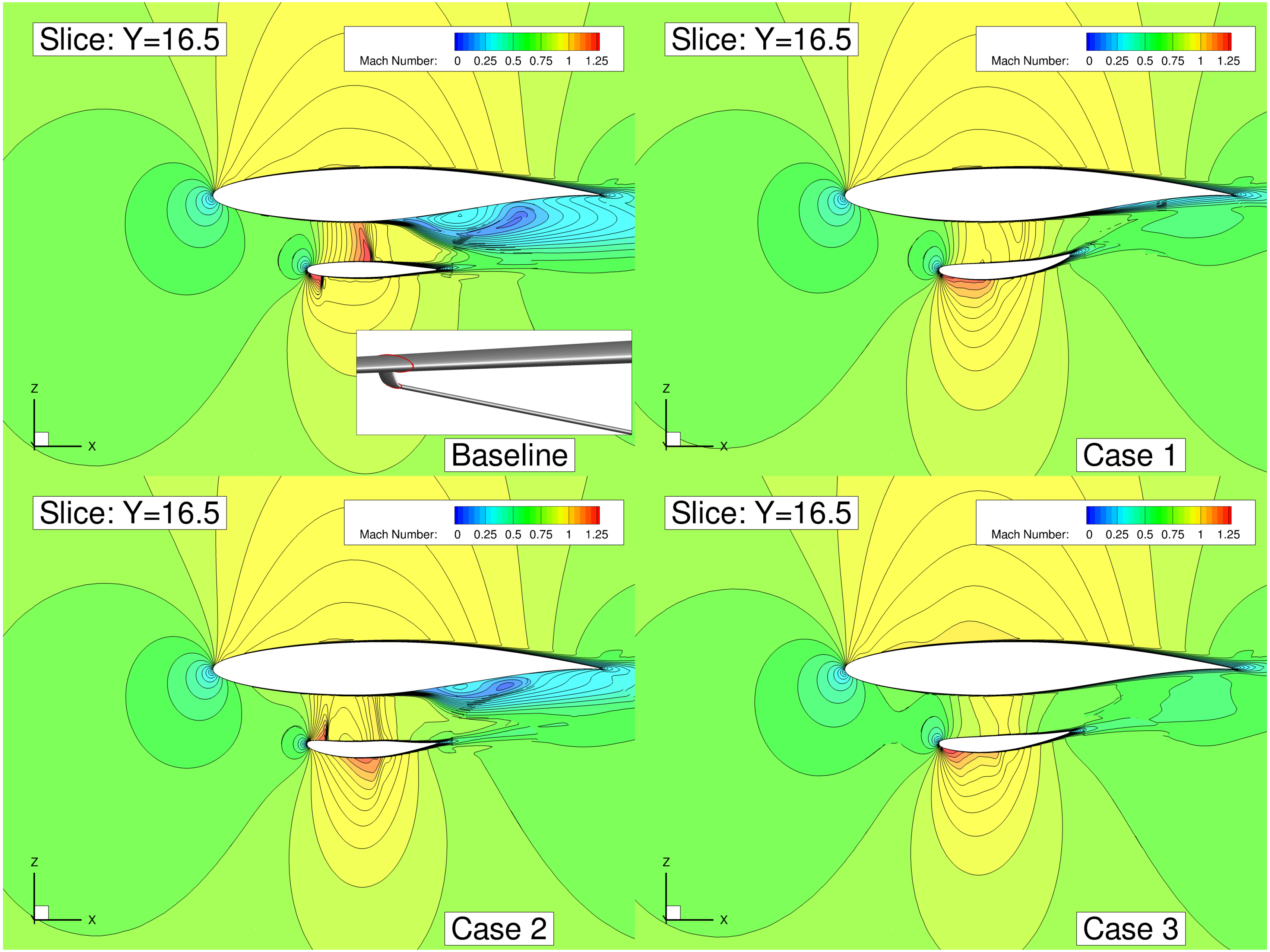

2D Slices of Junction Region

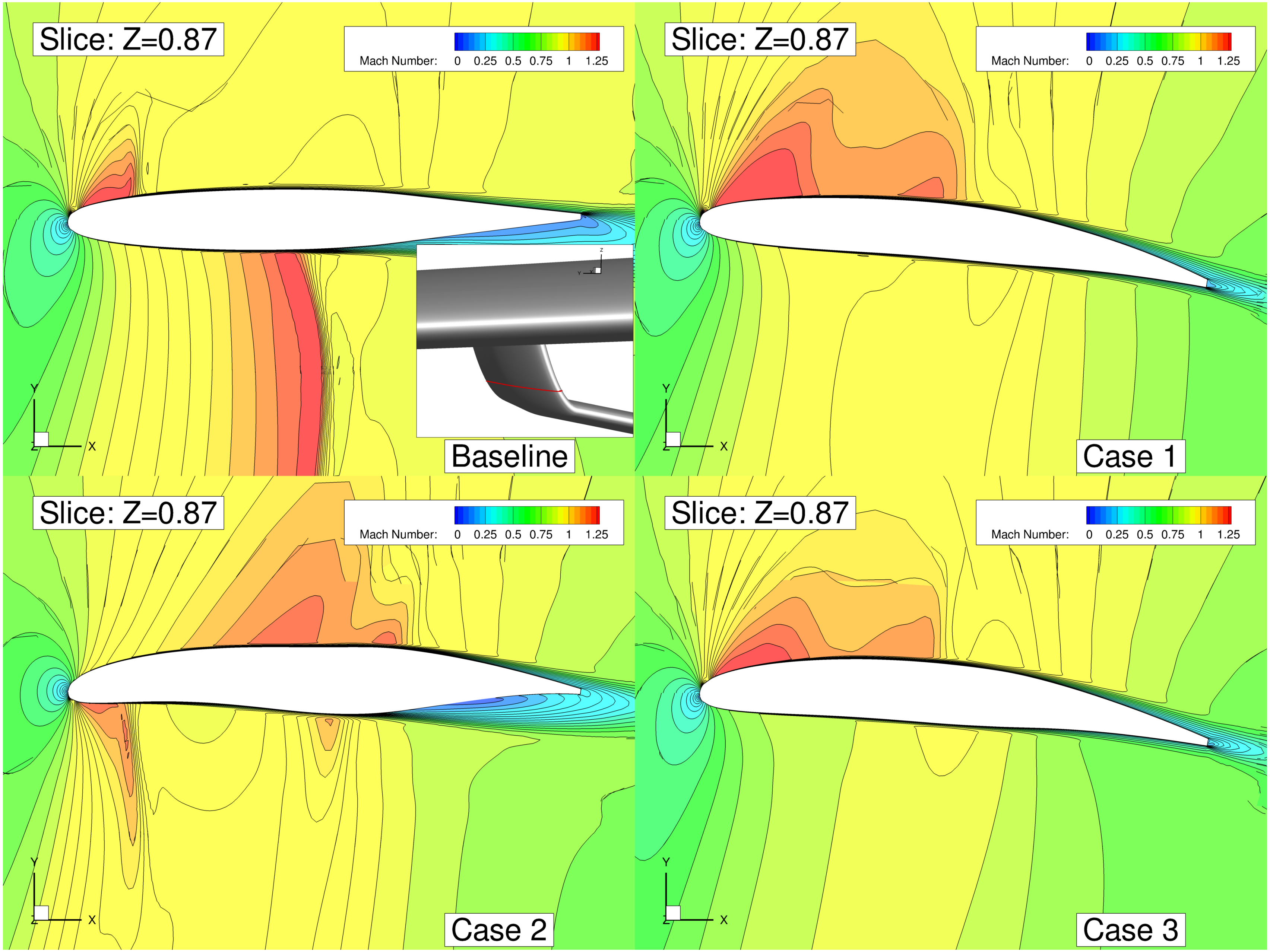

2D Slices of Junction Region

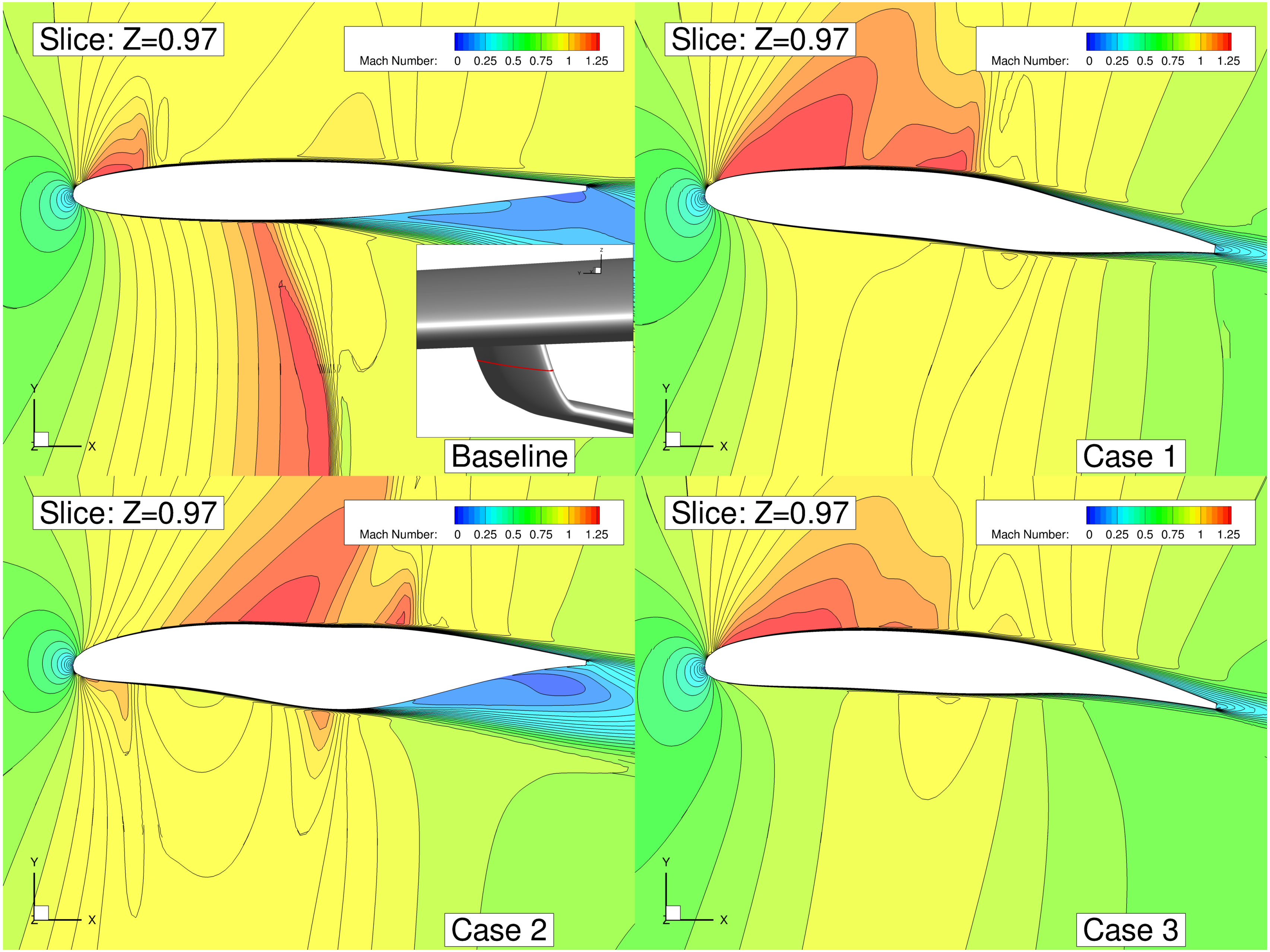

2D Slices of Junction Region

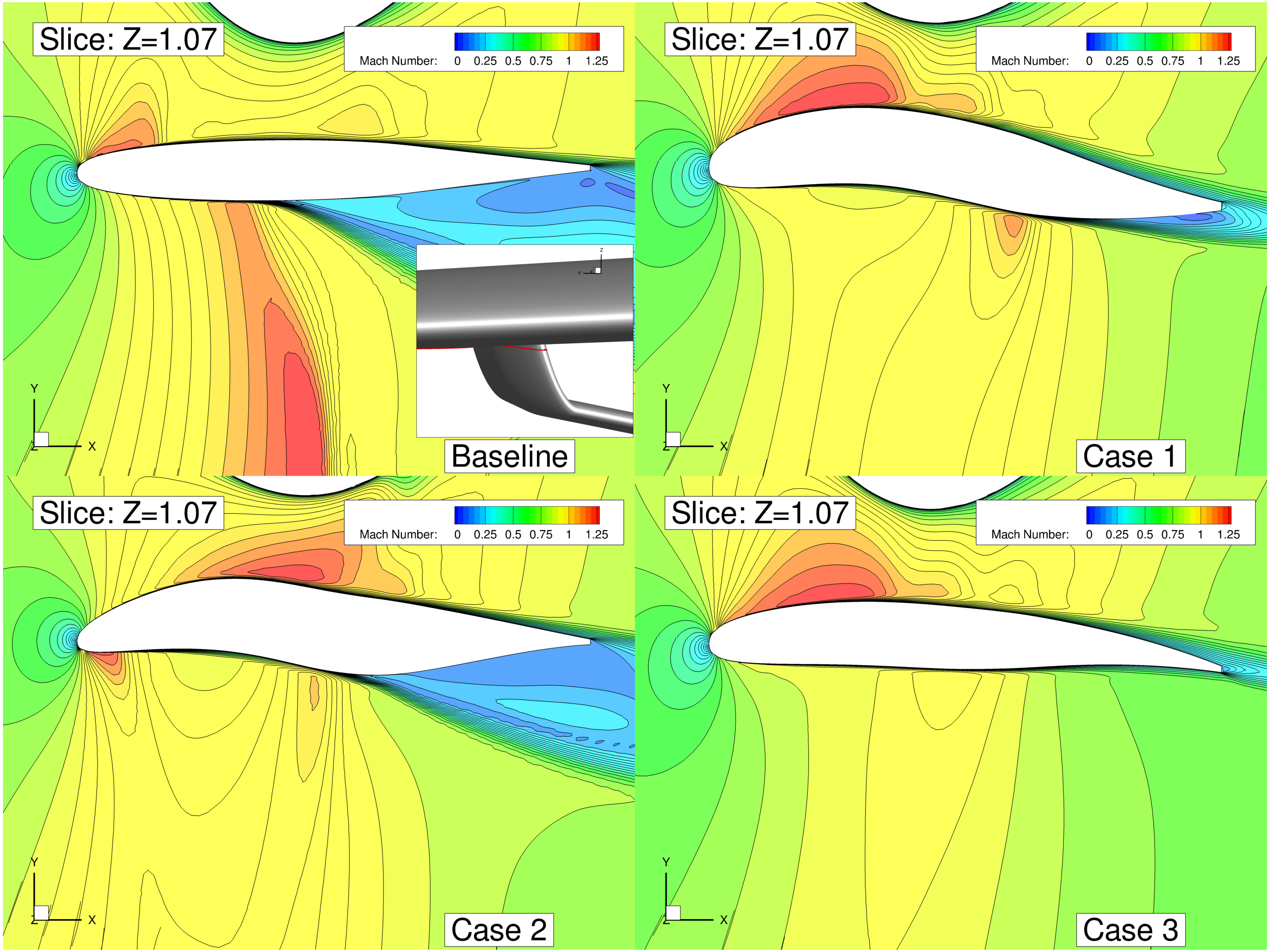

2D Slices of Junction Region

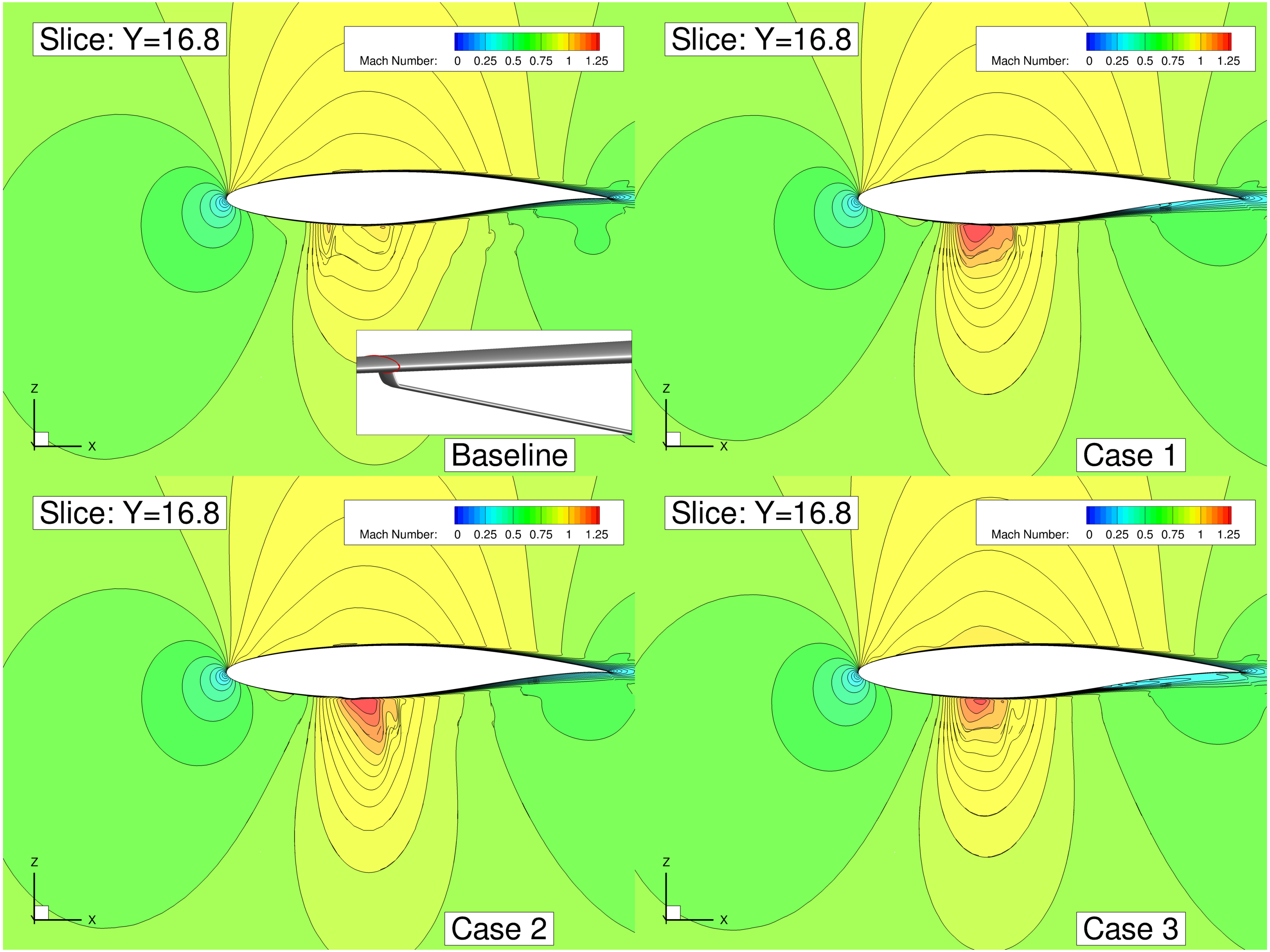

2D Slices of Junction Region

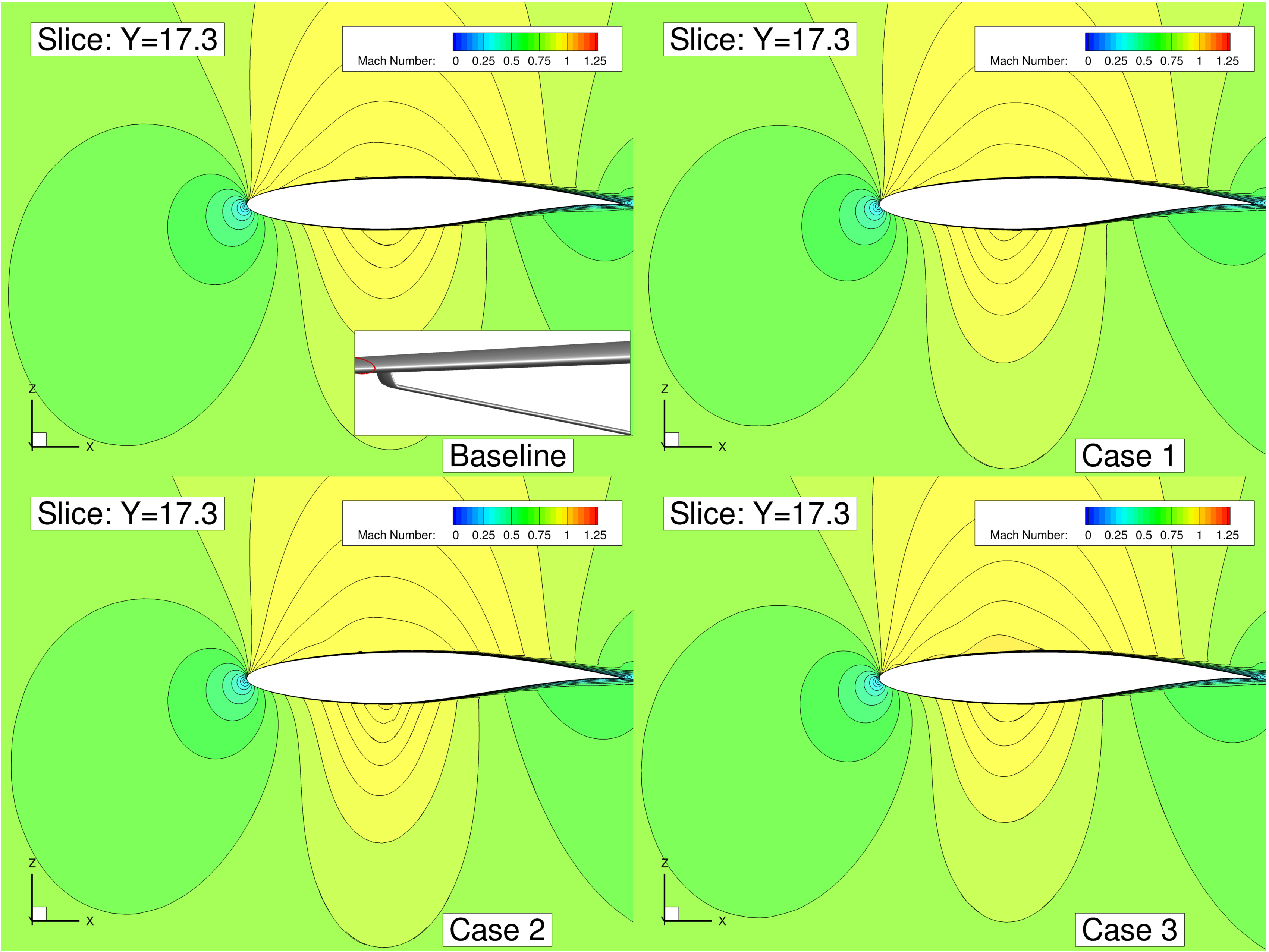

2D Slices of Junction Region

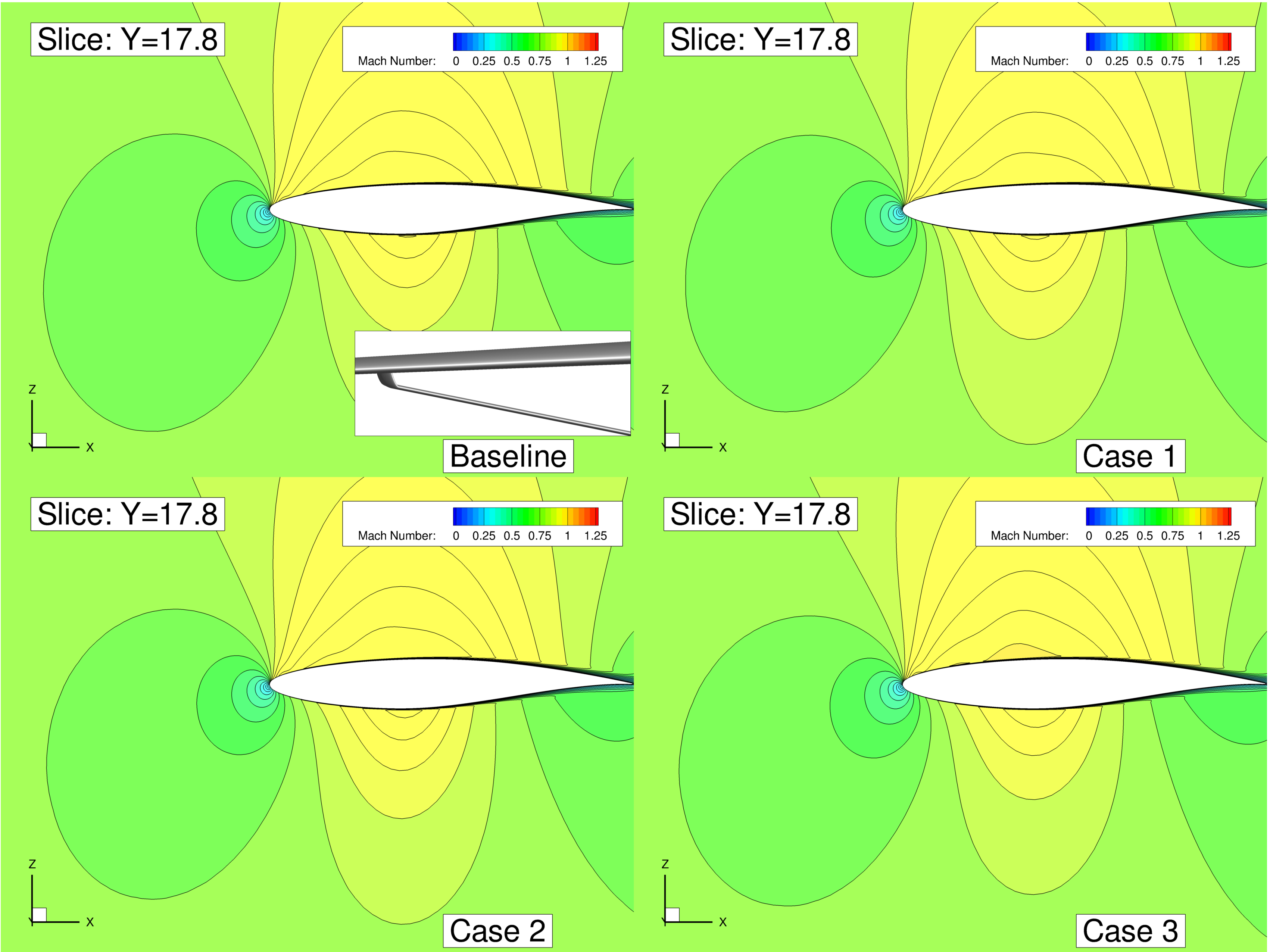

Shock Surface Visualization

- Case 1 successfully removes shock in design region
- Full truss redesign has weak shock on lower surface

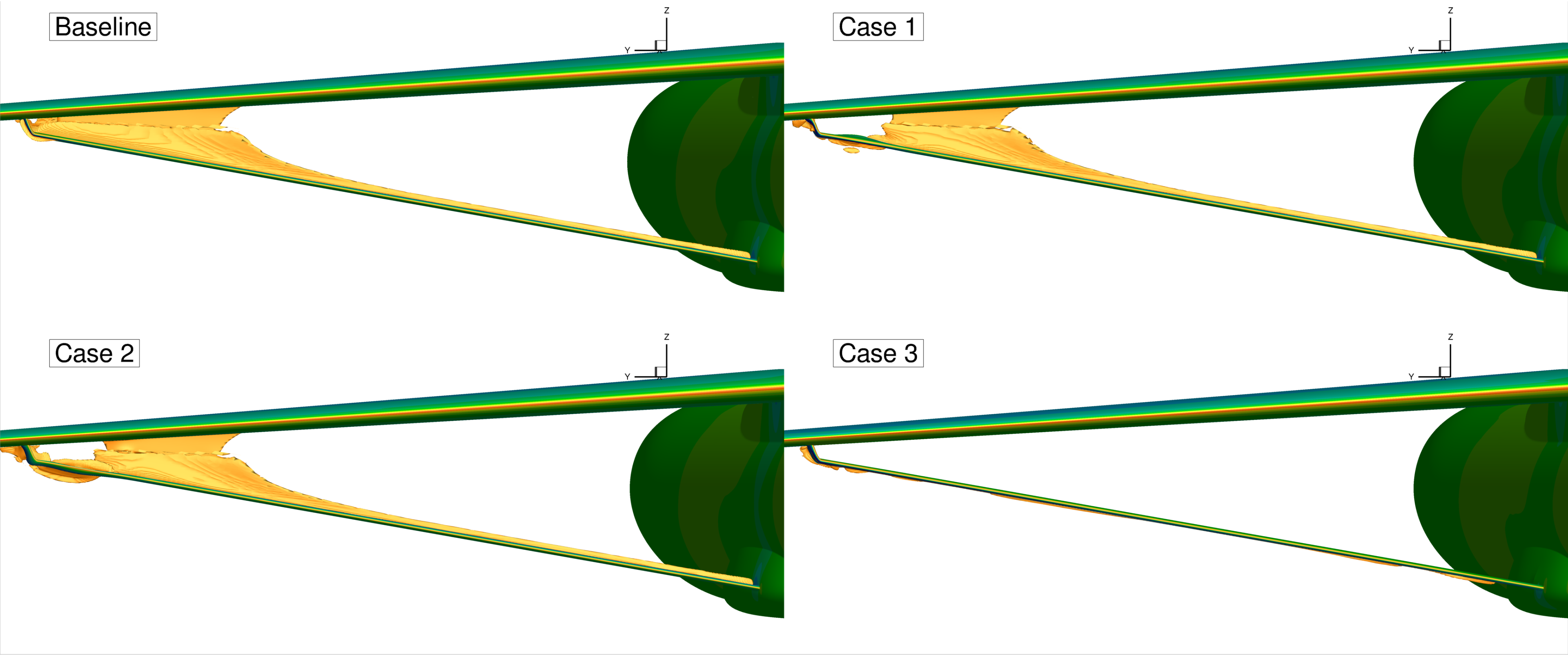

Separated Flow

- All designs reduce the amount of separated flow at the strut-wing junction
- Red iso-contour at Vx=-.0001

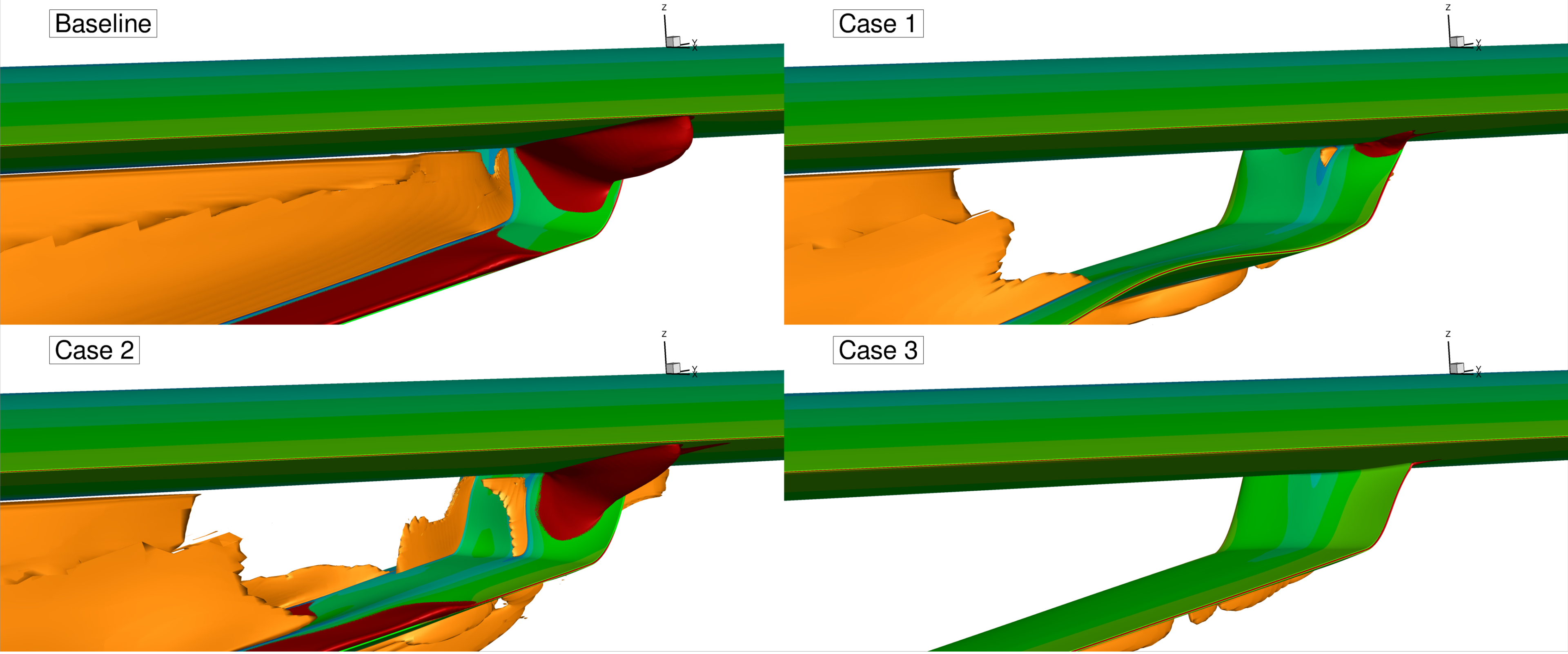

Separated Flow

- All designs reduce the amount of separated flow at the strut-wing junction
- Red iso-contour at Vx=-.0001

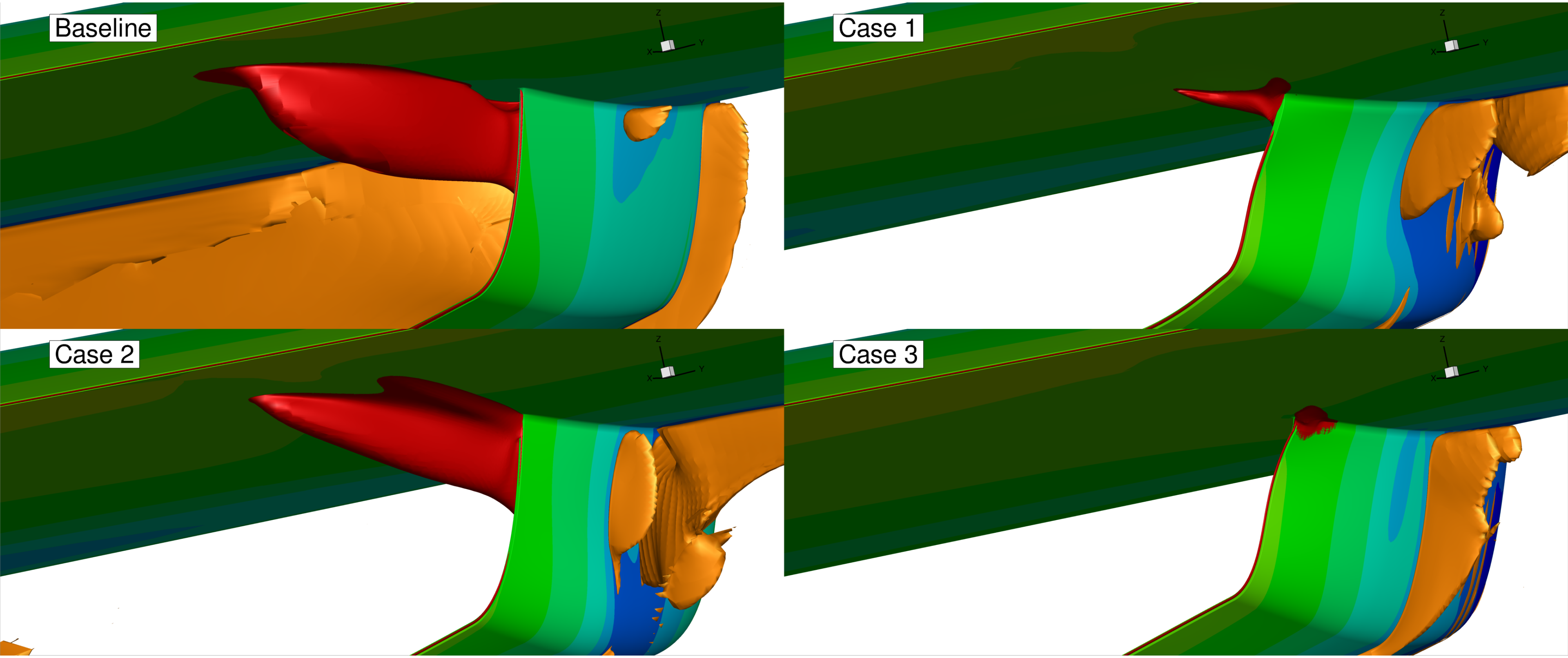

Lift Distributions

- All optimized designs reduce truss lift
- Nearly elliptical lift distribution and increased angle of attack for case 3
- Negative truss lift is optimal!

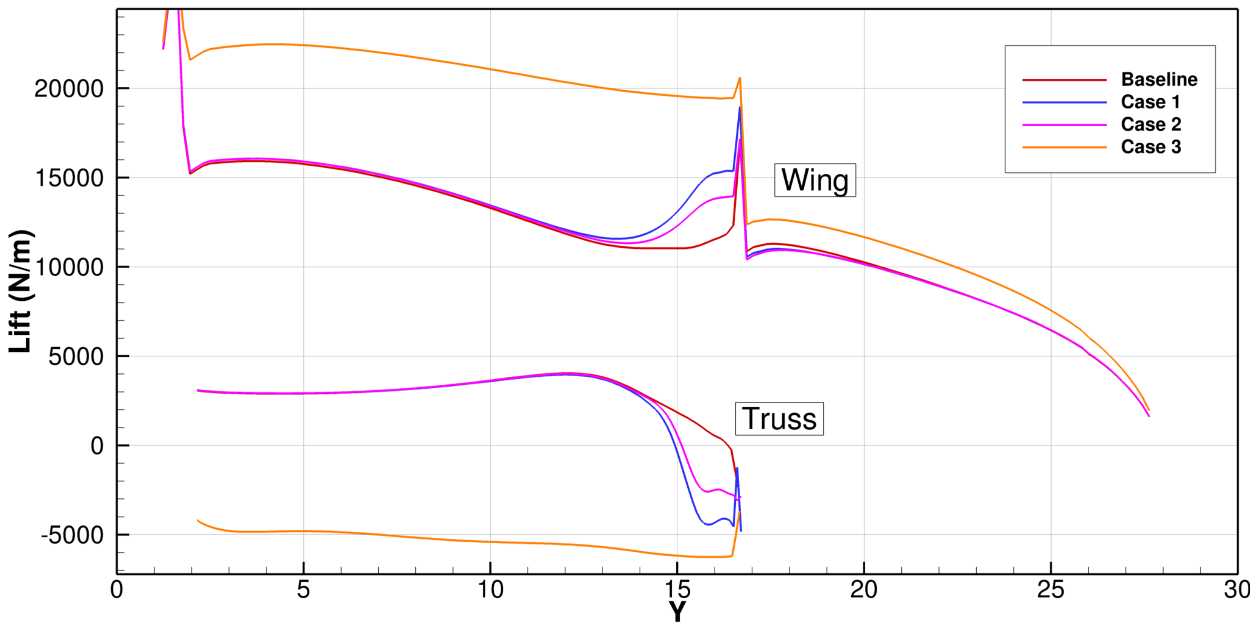

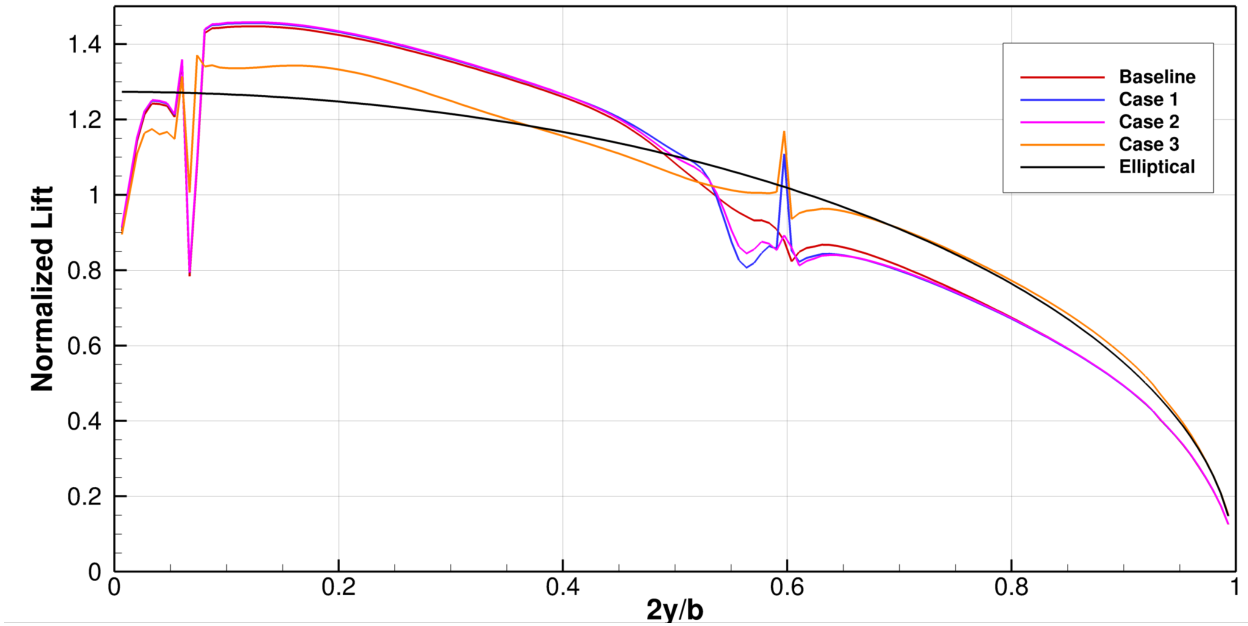

Off-Design Performance

- Consistent improvement across Mach and angle of attacks

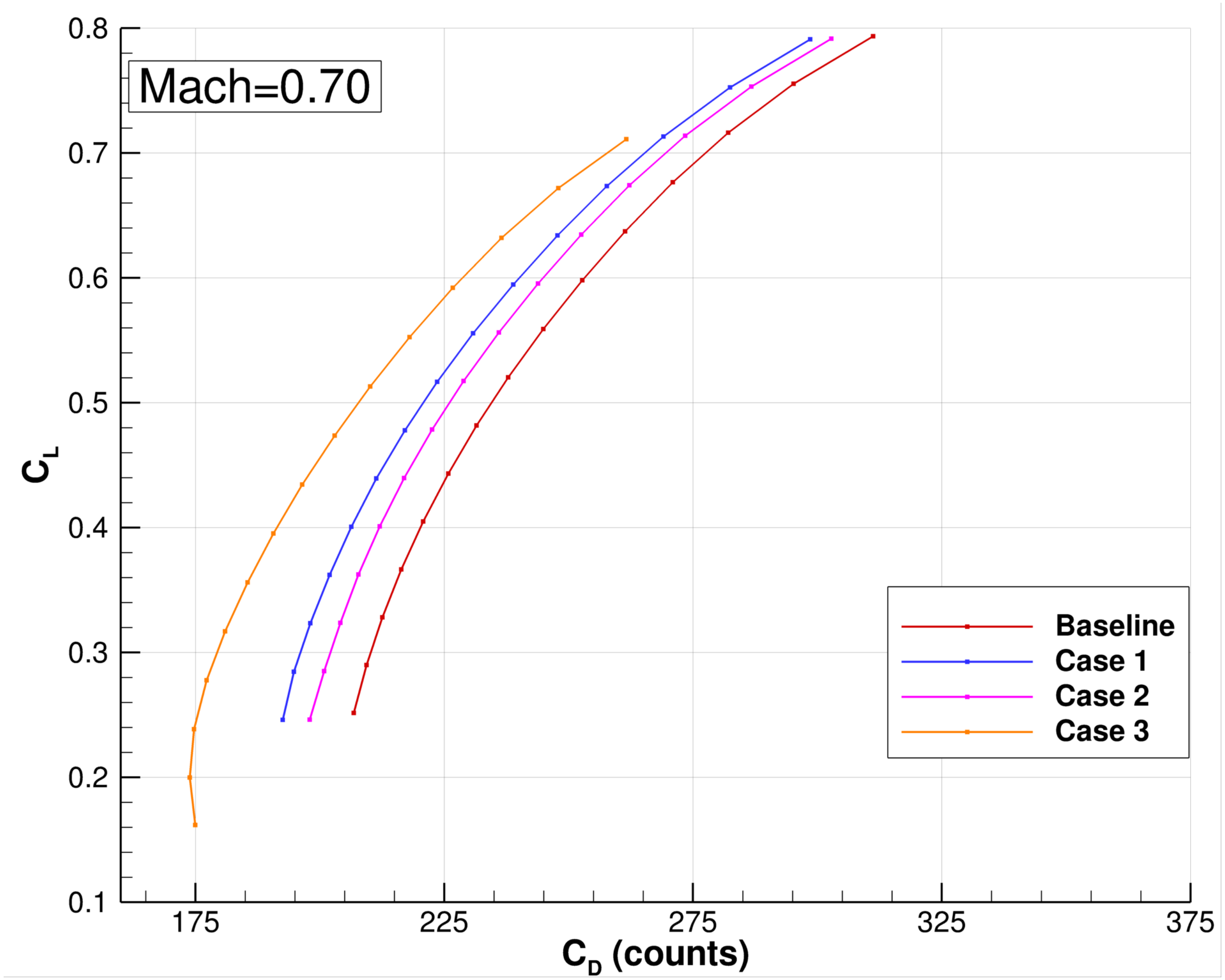

Off-Design Performance

- Consistent improvement across Mach and angle of attacks

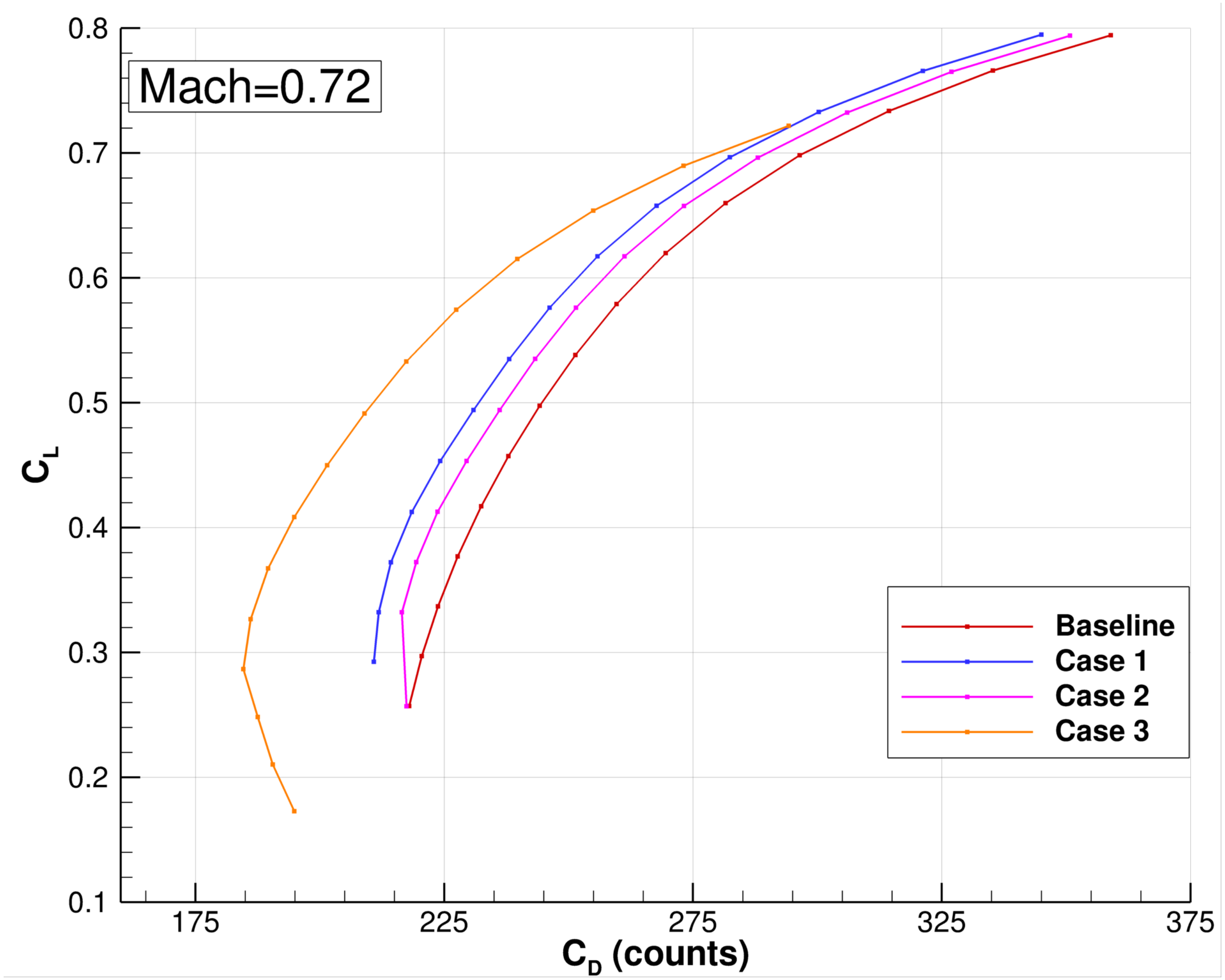

Off-Design Performance

- Consistent improvement across Mach and angle of attacks

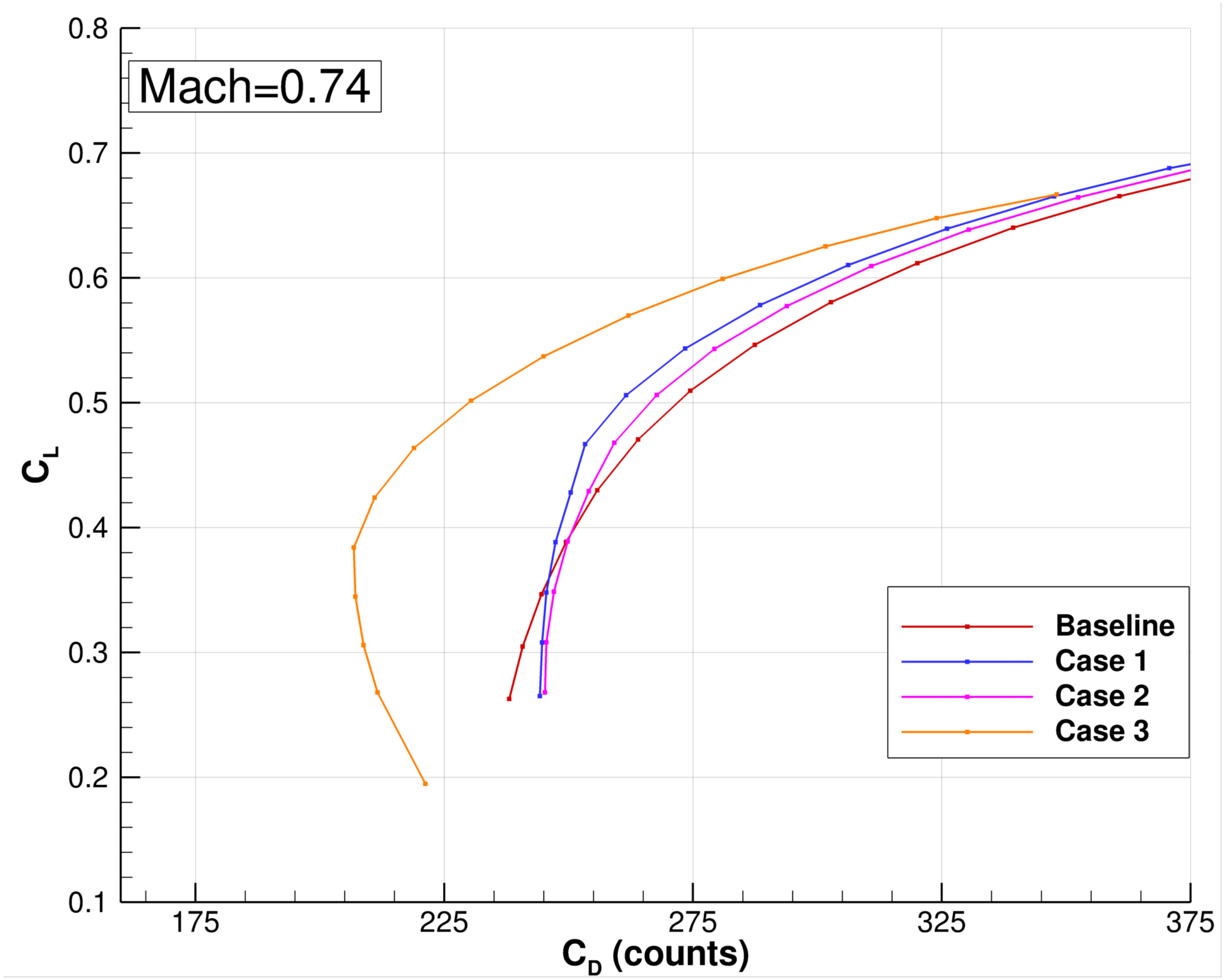

Optimization Case 1

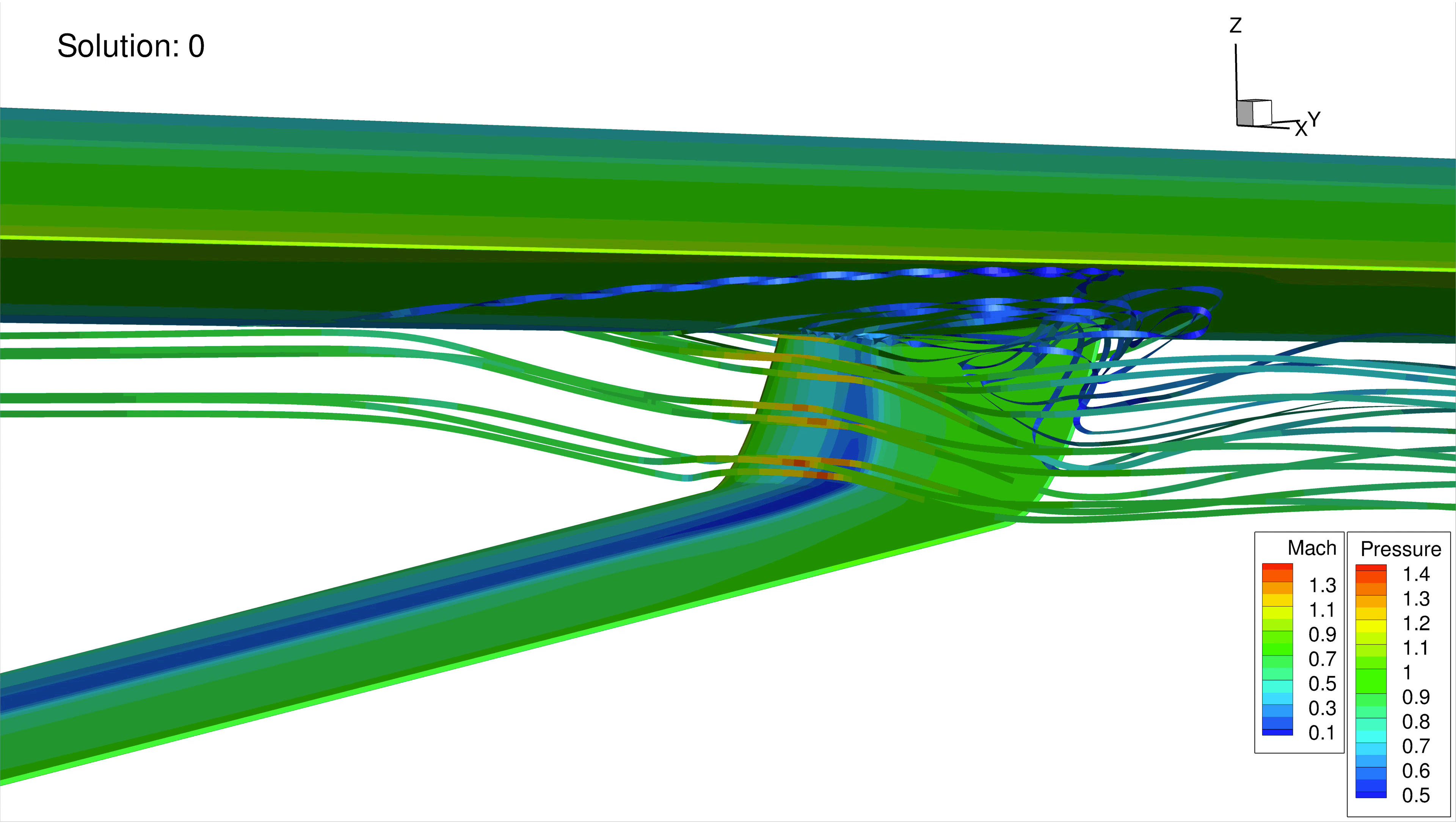

Pressure is shown on the surface. Stream ribbons are colored by Mach number.

Optimization Case 2

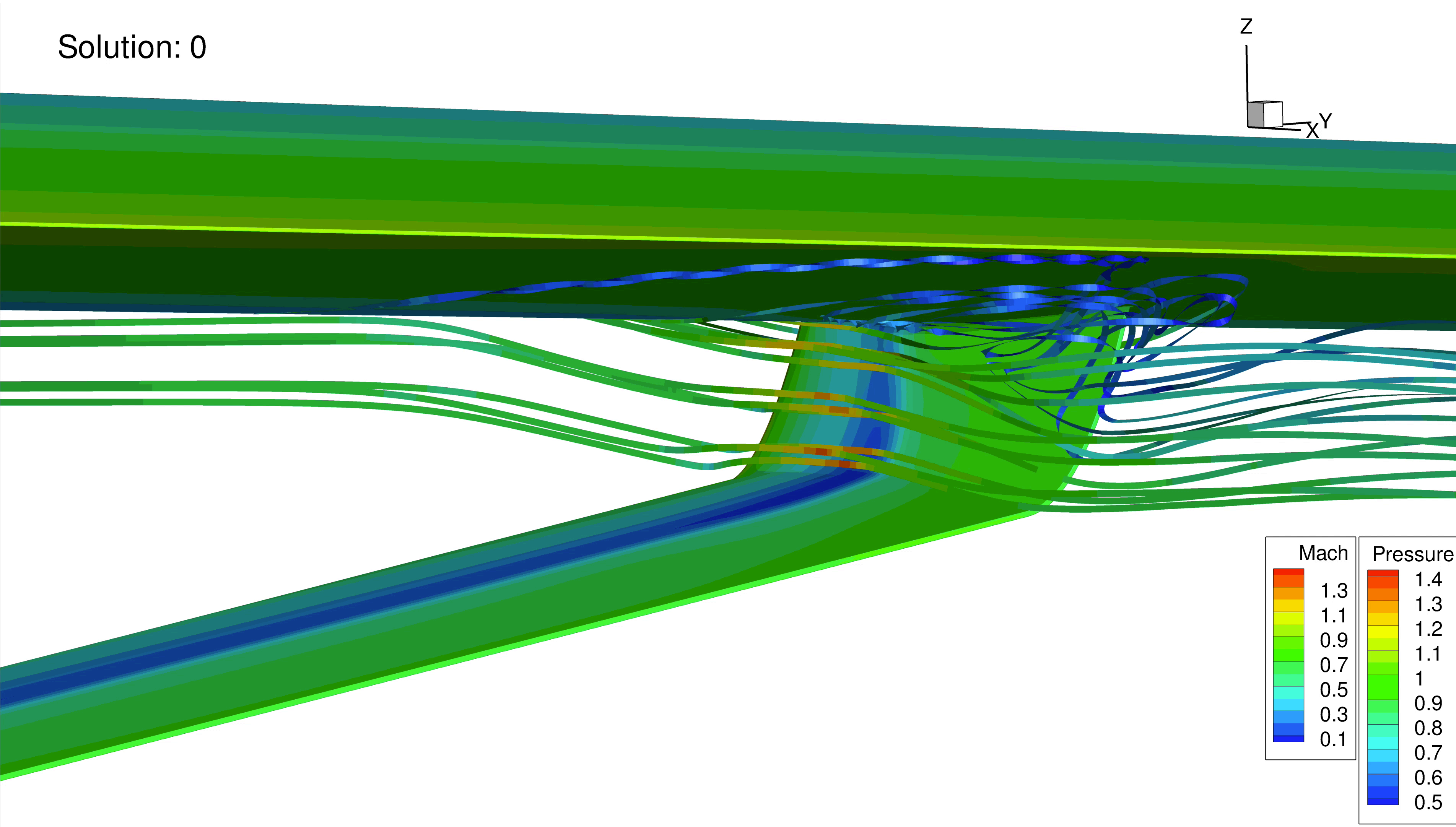

Pressure is shown on the surface. Stream ribbons are colored by Mach number.

Optimization Case 3

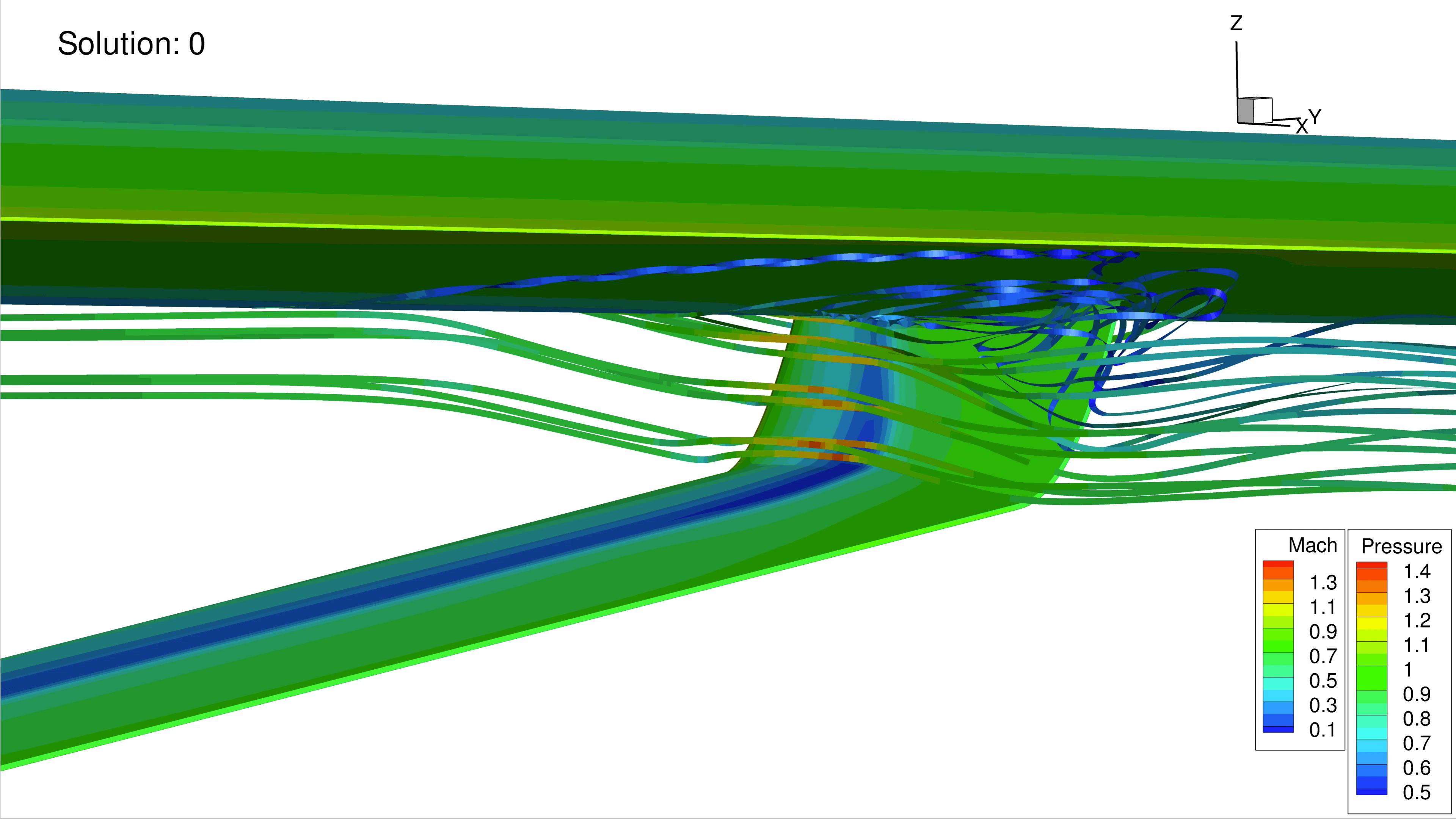

Pressure is shown on the surface. Stream ribbons are colored by Mach number.

Summary

- Successfully redesigned truss-junction intersection
- Fast optimization turn-around times of under 2 hours
- 13.5 drag count reduction for Case 1
- 33.5 drag count reduction for Case 3
- In transonic flow, truss may have negative lift
- No cost associated with flow control device other than initial development costs
- Future work should include aero-structural trade-offs

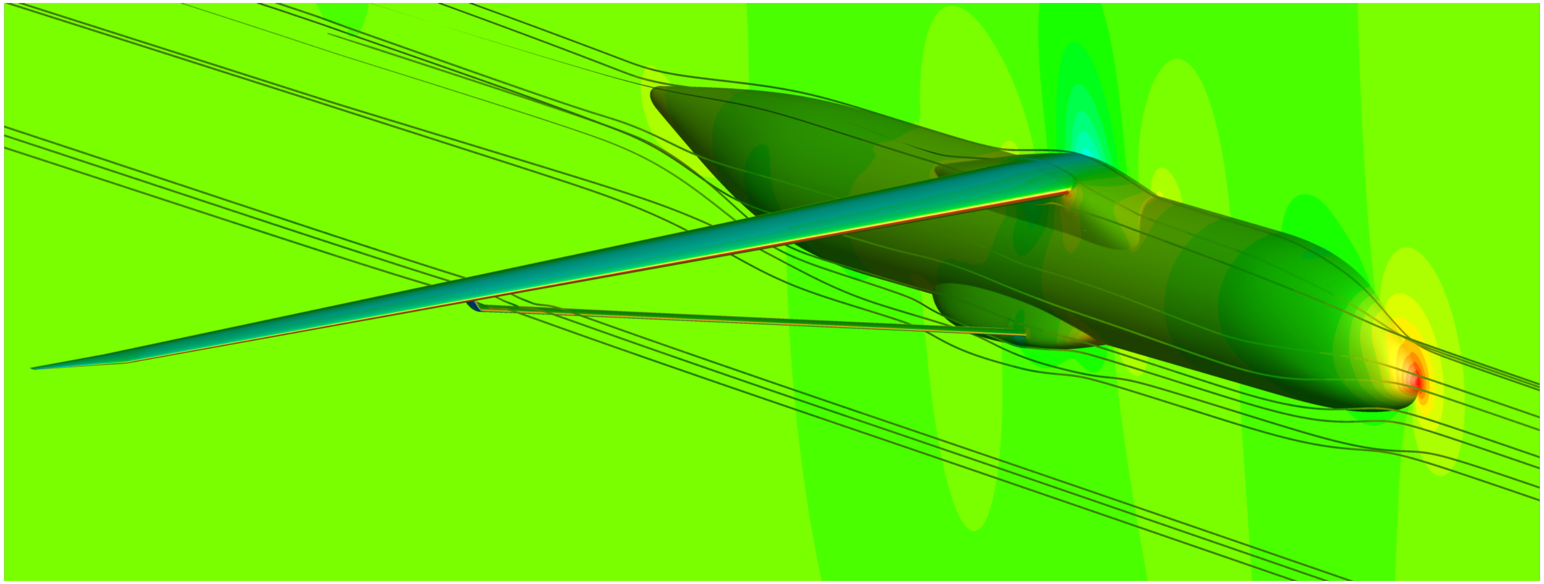

Questions

This work is funded by Nasa Advanced Air Transport Technology (AATT), sub project High Aspect Ratio Wing (HAW)